Editors' choice

A new gobiconodontid mammal from Upper Cretaceous of China and reassessment of dentition in *Gobiconodon*

WENHAO WU, FANGYUAN MAO, JUN CHEN, and JIN MENG

Wu, W., Mao, F., Chen, J., and Meng, J. 2026. A new gobiconodontid mammal from Upper Cretaceous of China and reassessment of dentition in *Gobiconodon*. *Acta Palaeontologica Polonica* 71 (2): 193–210.

We provide a detailed description of the dental morphology of *Gobiconodon zofiae* based on the holotype and clarify its diagnostic features in comparison with other species in the genus. We also report a new species, *Gobiconodon gongzhulingensis* sp. nov., from the lower Upper Cretaceous Quantou Formation in Gongzhuling City, Jilin Province, based on a maxilla with five molariforms. The dental morphologies of both species allow us to reassess tooth assignments in *Gobiconodon* and support a dental formula of 2.1.3.4/2.1.3.5 for the genus. The molariforms of *Gobiconodon* exhibit a distinct type of tooth widening that is achieved primarily through cusp inflation, without pronounced cusp rotation or the addition of new cusps. In addition to the differences in occlusal pattern, embrasure shearing dominated by an orthal power stroke, accompanied by a labiolingually directed component of relative displacement of the lower teeth during mastication also distinguishes *Gobiconodon* from other eutriconodontans, particularly triconodontids, suggesting an insectivorous and/or omnivorous diet for *Gobiconodon*. The tooth shapes and wear patterns described here indicate diverse ecomorphological specializations and species diversification within eutriconodontans.

Key words: Mammalia, Gobiconodontidae, morphology, Quantou Formation, Upper Cretaceous, Jilin Province.

Wenhao Wu [wenhao.wu@foxmail.com; ORCID: https://orcid.org/0000-0003-0970-9713], Jun Chen [cj@jlu.edu.cn; ORCID: https://orcid.org/0000-0003-1019-3881], College of Earth Sciences, Research Centre of Palaeontology and Stratigraphy, Dinosaur Evolution Research Center, Jilin University, Changchun 130061, Jilin Province, China.
Fangyuan Mao [maofangyuan@ivpp.ac.cn; ORCID: https://orcid.org/0000-0002-8208-3473] (corresponding author), Key Laboratory of Vertebrate Evolution and Human Origins, Institute of Vertebrate Paleontology and Paleoanthropology, Chinese Academy of Sciences, Beijing 100044, China; Division of Paleontology, American Museum of Natural History, New York, New York 10024, USA.
Jin Meng [jmeng@amnh.org; ORCID: https://orcid.org/0000-0002-3385-83833], Division of Paleontology, American Museum of Natural History, New York, New York 10024, USA; Earth and Environmental Sciences, Graduate Center, City University of New York, New York, 10016, USA.

Received 1 December 2025, accepted 24 March 2026, published online 25 April 2026.

Introduction

Eutriconodonta (Kermack et al. 1973) is a Mesozoic mammalian group characterized by a triconodont molariform pattern, with three main cusps aligned mesiodistally and a dentary bone lacking a postdentary trough. Comprehensive reviews of eutriconodontans have been done in several studies (Kielan-Jaworowska and Dashzeveg 1998; Kielan-Jaworowska et al. 2004; Gaetano and Rougier 2011). *Gobiconodon*, a diverse genus within eutriconodontans, includes approximately ten reported species with a wide paleogeographic distribution across China, Mongolia, Russia, and North America (Averianov et al. 2023). Species of *Gobiconodon* possess the basic triconodont tooth pattern, with some species displaying incipient triangulation of the primary cusps (Kielan-Jaworowska and Dashzeveg 1998; Sigogneau-Russell 2003; Butler and Sigogneau-Russell 2016; Kusuhashi et al. 2020). Unlike triconodontids, another subgroup of eutriconodontans that show cusp elongation, gobiconodontids are characterized by cusp inflation and tooth crown widening, especially in the upper molariforms, possibly indicating a different dietary preference.

Diverse interpretations of valid *Gobiconodon* species and their dental formulae (Jenkins and Schaff 1988; Kielan-Jaworowska and Dashzeveg 1998; Rougier et al. 2001; Li et al. 2003; Lopatin and Averianov 2015; Kusuhashi et al. 2016, 2020), complicate the establishment of a consistent genus diagnosis. The taxonomic affinity of some *Gobiconodon* species is uncertain. For example, *Gobiconodon luoianus* is considered a junior subjective synonym of *G. zofiae*

(Lopatin and Averianov 2015, but see Kusuhashi et al. 2016) and the attribution of *G. palaios* and *G. bathoniensis* has been questioned by Lopatin and Averianov (2015; see also Kusuhashi et al. 2016, 2020). Including or excluding these species in *Gobiconodon* affects the diagnostic features of the genus.

Uncertainty in tooth count and assignment further complicates diagnosis. For instance, the presence of i3 in *Gobiconodon* was used as a feature to differentiate it from *Meemannodon* (Meng et al. 2005) and *Repenomamus* (Li et al. 2001; Hu et al. 2005), but the incisor count of *Gobiconodon* varies from one to three in various studies (Jenkins and Schaff 1988; Kielan-Jaworowska and Dashzeveg 1998; Rougier et al. 2001; Li et al. 2003; Lopatin and Averianov 2015; Kusuhashi et al. 2016). As noted by Lopatin and Averianov (2015), the anterior dentition of *Gobiconodon* is unusual and its dental formula has been variously interpreted, rendering incisor count an unreliable diagnostic feature for *Gobiconodon*. Despite these changes, certain features, such as five molariforms and five to six premolariforms in the dentary, and replacement of molariforms are consistently recognized in *Gobiconodon* and are commonly used as diagnostic characteristics (Jenkins and Schaff 1988; Kielan-Jaworowska and Dashzeveg 1998; Rougier et al. 2001). Some diagnoses for the genus include these features, although some, like the replacement of anterior molariforms, are probably plesiomorphic (Rougier et al. 2001).

A major challenge in species recognition of *Gobiconodon* is the bias on morphologies of lower teeth (Jenkins and Schaff 1988). This is a common issue in the study of Mesozoic mammals because the maxilla bone is more fragile and thinner than the mandible, leading lower jaws and teeth to more resistance to transport and wear. Consequently, our understanding of Mesozoic mammals primarily relies on mandibular and lower molariform morphology (Rougier et al. 2003). However, some species, such as *G. bathoniensis* and *G. palaios* are identified solely based on isolated upper teeth (Sigogneau-Russell 2003; Butler and Sigogneau-Russell 2016). In studies of *G. borissiaki* and *G. hoburensis* (Trofimov 1978; Kielan-Jaworowska and Dashzeveg 1998; Lopatin and Averianov 2015), researchers have recognized various mandibular and lower tooth features in diagnoses while omitting diagnostic features from the upper teeth. Conversely, some *Gobiconodon* species, such as *G. hopsoni*, are based on upper teeth as the holotype (Rougier et al. 2001), or, like *G. palaios* and *G. bathoniensis*, rely exclusively on isolated upper teeth (Sigogneau-Russell 2003; Butler and Sigogneau-Russell 2016). The association between upper and lower tooth morphologies in the genus remains largely uncertain. In this context, specimens with relatively complete and associated upper and lower dentitions from the same individual are critical for correlating dental morphology and confirming the tooth formula of *Gobiconodon*.

The holotype of *Gobiconodon zofiae*, with relatively complete and associated upper and lower dentitions from the same individual, provides critical evidence for interpreting tooth count and diagnostic features of *Gobiconodon*. Although *G. zofiae* was previously described by Li et al. (2003), the description and illustration of the tooth morphology was insufficient, leading to unclear diagnostic features and provisional species identification (Lopatin and Averianov 2015). In this study, with the support of high-resolution micro-CT scan images, we provide additional dental morphological information and interpretations for *G. zofiae*. The additional information presented here based on upper and lower teeth in association helps with identifying other *Gobiconodon* dental remains, enhancing our understanding of the diversity of this genus. Additionally, we revise the diagnosis of *Gobiconodon* by incorporating more upper dental features, particularly the holotype of *G. zofiae* (Li et al. 2001).

We also describe a new gobiconodontid species *Gobiconodon gongzhulingensis* sp. nov. from the Quantou Formation (lower Upper Cretaceous, Cenomanian–middle Turonian; Wan et al. 2013; Wang et al. 2016, 2022b; Xi et al. 2019), Shanqian Village, Liufangzi Town, Gongzhuling City, Changchun Area, Jilin Province, northeast China (Yang et al. 2023, Fig. 1). Based on the new information derived from the two *Gobiconodon* species, we discuss the tooth assignments and dental formula of *Gobiconodon*, and tooth widening of *Gobiconodon*, in comparison to other triconodontid tooth patterns.

Institutional abbreviations.—HGM, Henan Geological Museum, Zhengzhou, China; IVPP, Institute of Vertebrate Paleontology and Paleoanthropology, Chinese Academy of Sciences, Beijing, China; LACM, Natural History Museum, London, UK; PIN, Borissiak Paleontological Institute, Russian Academy of Sciences, Moscow, Russia; PSS, Paleontological and Stratigraphic Section, Institute of Geology, Mongolian Academy of Sciences, Ulan Bator, Mongolia; RCPS, Research Centre of Palaeontology and Stratigraphy, Jilin University, Changchun, Beijing, China.

Nomenclatural acts.—This published work and the nomenclatural acts it contains have been registered in ZooBank: urn:lsid:zoobank.org:act:006164BE-8715-4C70-A792-B02152E8A905.

Geological setting

The Songliao Basin is a large continental rift basin covering approximately 260 000 km^2 in northeastern China (Wan et al. 2013; Zhu et al. 2020). The basin is primarily filled with nearly continuous Cretaceous sediments, reaching a total thickness of ~10 km (Wang et al. 2020). The Cretaceous strata are divided into nine formations (from bottom to top): Shahezi (K_1s), Yingcheng (K_1y), Denglouku (K_1d), Quantou (K_2q), Qingshankou (K_2qn), Yaojia (K_2y), Nenjiang (K_2n), Sifangtai (K_2s) and Mingshui (K_2m) formations (Wang et al. 2022b; Fig. 1).

The Quantou Formation is subdivided into four members, consisting primarily of brownish-red, purple-brown

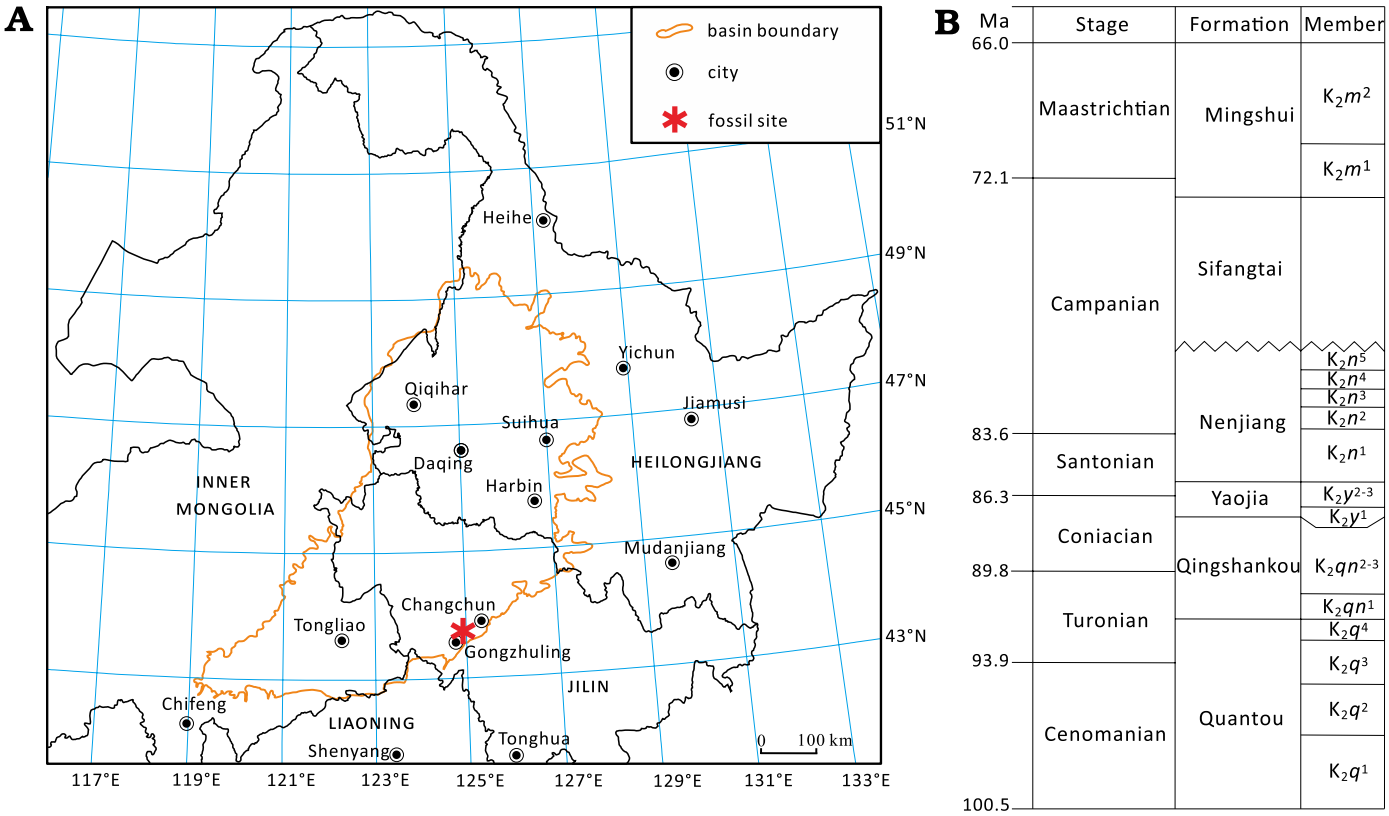

Fig. 1. The fossil locality map for *Gobiconodon gongzhulingensis* sp. nov. (**A**) and the Cretaceous strata of the Songliao Basin (**B**) in central Jilin Province, northeastern China (according to Yang et al. 2023).

and grayish-green mudstone, and sandstone, reflecting fluvial, lakeshore and shallow lake facies (Wang et al. 2009). Earlier studies suggested that the Quantou Formation spans the Albian to Cenomanian stages (Wang et al. 1996; Huang et al. 1999). However, recent high-precision CA-ID-TIMS geochronological studies indicate that the top of the Yingcheng Formation is dated to 102.571 Ma (Wang et al. 2022b), and the base of the Qingshangkou Formation to 91.886 Ma (Wang et al. 2016). These findings suggest that the Quantou Formation corresponds to the lower Upper Cretaceous, specifically the Cenomanian to middle Turonian stages (Wang et al. 2022b). We propose that the new gobiconodontid material described herein from the fourth member of the Quantou Formation dates to approximately early to middle Turonian (Wan et al. 2013; Xi et al. 2019; Wang et al. 2016, 2022b).

The Shanqian fossil locality from Gongzhuling City (Fig. 1), has yielded multiple vertebrate fossils, including ornithopods (Chen et al. 2008, 2018; Jin et al. 2010), ceratopsians (Jin et al. 2009), theropods (Zan et al. 2003; Wang 2005), sauropods (Wu et al. 2006), dinosaur eggshells (Wang et al. 2006), and crocodyliforms (Zan et al. 2003). This vertebrate fossil assemblage was named the *Changchunsaurus* fauna (Wang et al. 2022a). The zalambdalestid *Zhangolestes jilinensis* was reported from this locality (Zan et al. 2006; Chen et al. 2025), and undescribed therian remains are known from Shanqian. Because this fauna is probably younger than the Jehol and Fuxin biotas but older than the Late Cretaceous faunas in the Gobi Desert area (Jerzykiewicz et al. 1993; Kielan-Jaworowska et al. 2003; Xu et al. 2013), it furnishes critical information on the evolution of vertebrates in general. The new eutriconodontan species reported here increases the diversity of mammals from this fauna and enhances our knowledge about the evolution of *Gobiconodon.*

Material and methods

Material.—The holotype specimen of *Gobiconodon zofiae* (IVPP V12585) from Jehol biota, is a partial skull with associated mandibles and almost complete upper and lower dentition. The holotype of *Gobiconodon gongzhulingensis* sp. nov. (RCPS VJ8001), a right maxilla fragment with five postcanine teeth, was discovered from the matrix fragments chiseled off while preparing dinosaur specimens from the locality at Gongzhuling City.

Images, SEM and CT-scans.—The conventional photographs of *Gobiconodon zofiae* (IVPP V12585) were taken using a Canon Digital camera attached to a macro lens. The SEM photographs of the holotype of *Gobiconodon gongzhulingensis* (RCPS VJ8001) were taken without coating using a Hitachi S-3700N scanning electron microscope at the

Key Laboratory of Vertebrate Evolution and Human Origin, IVPP. The SEM photographs were taken at 3–5 kV voltage and with magnifications between 12× and 95× for studying tooth morphology and wear patterns.

High-resolution micro-computed tomography (μCT) was used to investigate both specimens. *Gobiconodon gongzhulingensis* (RCPS VJ8001) was scanned using a GE v|tome|x m300&180 μCT system (GE Measurement & Control Solutions, Wunstorf, Germany). The scan was performed with the 180 kV microfocus X-ray tube at an accelerating voltage of 130 kV and a current of 90 μA, achieving a voxel resolution of 5.91 μm. A total of 2000 projections were acquired, each with an exposure time of 1000 ms, and averaged twice to improve the signal-to-noise ratio. The raw projection data were reconstructed using Phoenix datos|x software (General Electric, Wunstorf, Germany).

Gobiconodon zofiae (IVPP V12585) was scanned using a 225 kV micro-computed tomography system developed by the Institute of High Energy Physics, Chinese Academy of Sciences, and housed at the Key Laboratory of Vertebrate Evolution and Human Origins, Chinese Academy of Sciences (Beijing, China). Scanning was conducted at an accelerating voltage of 120 kV and a beam current of 120 μA, resulting in a voxel resolution of 29.8 μm. The scans were done with a 360° rotation with a step increment of 0.5° and an unfiltered aluminum reflection target. A total of 720 transmission images were reconstructed in a 2048×2048 matrix of 1536 slices. Segmentation, three-dimensional reconstruction, and rendering of the CT data were performed using VGStudio Max 3.5 (Volume Graphics, Heidelberg, Germany).

Terminology.—We follow Jenkins and Schaff (1988) and Rougier et al. (2001, 2007) in using the terms premolariform and molariform for postcanine teeth and Crompton and Jenkins (1968) for cusp terminology. The tooth formula of gobiconodontids has been variably interpreted across studies. The lower dentition, which is based on a much better fossil record than the upper one and thus commonly used, ranges from 1.1.4.5 (Jenkins and Schaff 1988; Kielan-Jaworowska and Dashzeveg 1998; Maschenko and Lopatin 1998; Li et al. 2003; Kielan-Jaworowska et al. 2004), 2.1.2-3.5 (Meng et al. 2005; Kusuhashi et al. 2016; Yuan et al. 2009), and 3.1.2.5 (Rougier et al. 2007; Lopatin and Averianov 2015); the latter two formulae are possible for the antemolariforms. All these studies recognize the presence of five lower molariforms in gobiconodontids. While five upper molariforms were commonly considered in gobiconodontids, four upper molariforms were recognized in *G. zofiae* and *Repenomamus* (Li et al. 2003; Hu et al. 2005; Meng et al. 2005; Kusuhashi et al. 2016), which we adopt and further discuss in this study. We follow Lopatin and Averianov (2015) in recognizing the tooth generations and wherever possible denote the second generation (or replaced) tooth with "R/r" after the molariform number. For instance, M1R represents the replaced first upper molariform. However, we define "molariform" as a descriptive term referring to crown morphology, not homology. Tooth generations can be inferred from the relative tooth wear in the dentition and CT image of the roots and tooth germ in the jawbone. Due to uncertainty regarding tooth homology and loss across species of *Gobiconodon*, the designation of a tooth locus, such as P1, does not necessarily imply homology.

Systematic palaeontology

Mammalia Linnaeus, 1758

Eutriconodonta Kermack et al., 1973

Gobiconodontidae Chow & Rich, 1984

Genus *Gobiconodon* Trofimov, 1978

Type species: *Gobiconodon borissiaki* Trofimov, 1978; Khoboor locality in the Guchin Us Soinon County, Gobi Desert, Mongolia, Khoboor beds, Aptian–Albian, Early Cretaceous.

Species included: *Gobiconodon hoburensis* Trofimov, 1978, *Gobiconodon hopsoni* Rougier et al., 2001, *Gobiconodon ostromi* Jenkins & Schaff, 1988, *Gobiconodon zofiae* Li et al., 2003, *Gobiconodon tomidai* Kusuhashi et al., 2016, *Gobiconodon haizhouensis* Kusuhashi et al., 2016, *Gobiconodon gongzhulingensis* sp. nov.; *Gobiconodon luoianus* Yuan et al., 2009, *Gobiconodon palaios* Sigogneau-Russell, 2003, and *G. bathoniensis* Butler & Clements, 2001, *Gobiconodon* spp.

Emended diagnosis.—Dental formula 2.1.2-3.4/2.1.2-3.5; the lower mesial incisor (presumably i1) enlarged and procumbent at different degrees; posterior incisors, canines, and anterior premolariforms single-rooted and similar in morphology; the ultimate premolariforms in the upper and lower dentition (probably deciduous teeth) smaller than other postcanines or absent; anterior molariform undergone replacement; molariforms (particularly the upper) transversely widened with labiolingually directed component of relative displacement occlusion; two foramina of the infraorbital canals with the anterior foramen significantly larger.

Gobiconodon zofiae Li et al., 2003

Figs. 2, 3, 7.

Type material: IVPP V12585, a partial skull (a skull, with right half damaged, and associated lower jaws, Li et al. 2003: text-fig. 1).

Type locality: Lujiatun village, Shanyuan, Beipiao City, Liaoning Province, China.

Type horizon: Fist Member of the Yixian Formation, Lower Cretaceous, Barremian–Aptian.

Emended diagnosis.—Dental formula 2.1.3.4/2.1.3.5. The alveolus ridge is distinct. Strong double-rooted P2 and a small and single-rooted P1; a small diastema between each pair of adjacent teeth from i2 to dp3. Differs from *Gobiconodon borissiaki* in having a strong double-rooted P2 and a more reduced dP3 (in our interpretation, but M1 in others); similar to *G. ostromi and G. hoburensis* but differs from *G. borissiaki* in having i1 notably larger (twice in size) than i2 and the lower canine. Differs from *G. hoburensis* in have a double-rooted dp3 (dp2 in others; Lopatin and Averianov 2015: figs. 13, 14; note that this tooth was labeled as p2) and the

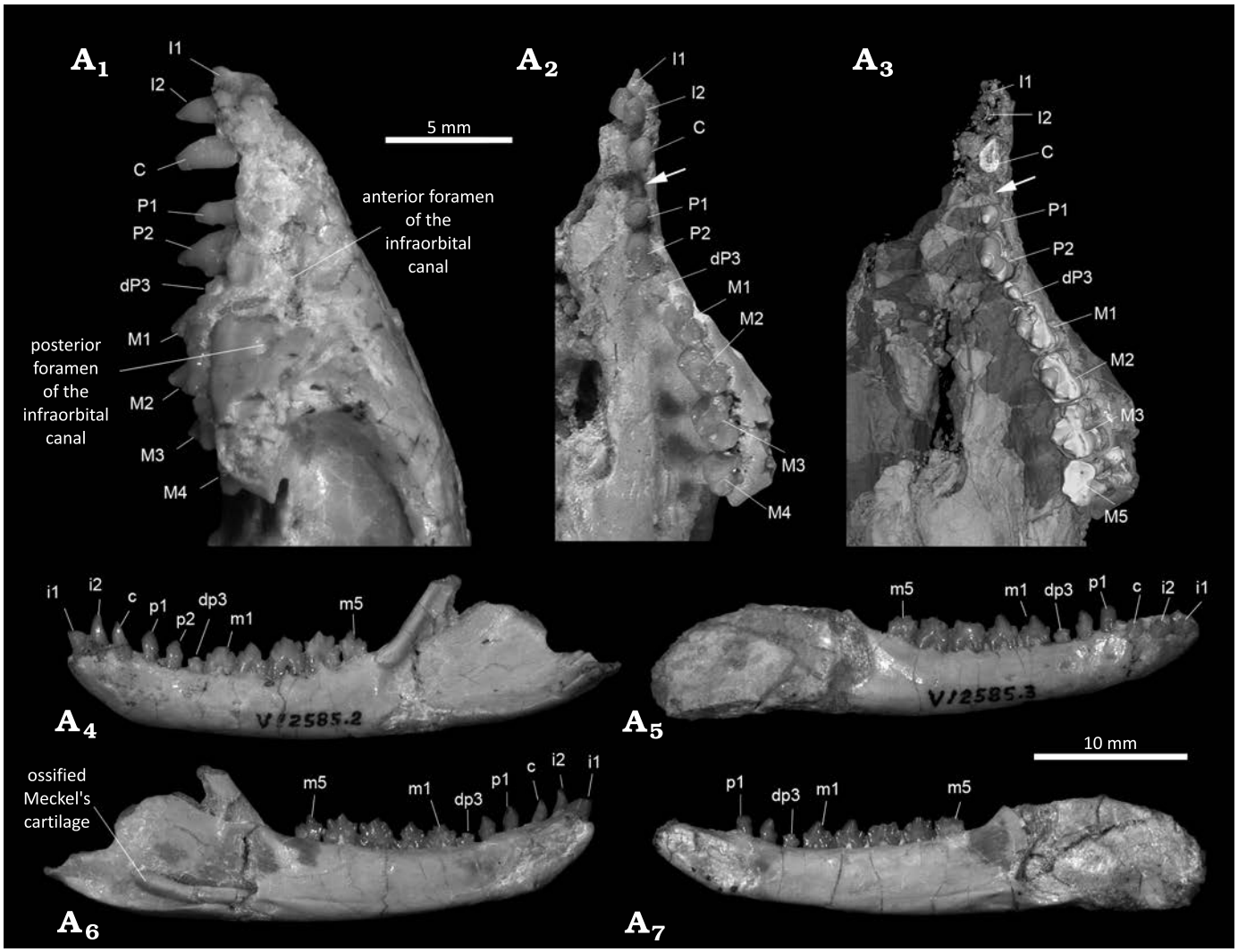

Fig. 2. Cranium and jaws of the gobiconodontid mammal *Gobiconodon zofiae* Li et al., 2003, holotype (IVPP V12585) from Lower Cretaceous of Lujiatun, Beipiao, China. Anterior portion of the cranium in left lateral (A_1) and ventral (A_2, A_3) views (A_2, photograph; A_3, 3D-rendering of CT data, emphasizing the dentition); left lower jaw in lateral (A_4) and medial (A_5) views; right lower jaw in lateral (A_6) and medial (A_7) views. Arrows point to the diastema between the upper canine and P1.

anterior teeth (from i2 to dp3) are separated by a narrow gap; p1 and p2 with a simple crown. Differs from *G. ostromi* and *G. hopsoni* in being smaller; mandible shallow posteriorly (without anterior tapering in lateral view), masseteric fossa smaller and not anteriorly extended; i2, canine, and p1 weaker and not conical; lower molariform cusp a is less mesially positioned; upper molariforms with wider cingulum; i1 less procumbent. Differs from *G. palaios* and *G. bathoniensis* in having a more rectangular outline of the upper molariforms and a less triangular arrangement of the main cusps. Differs from *G. tomidai* in being larger and having one more lower premolariform, a diastema between adjacent anterior teeth, and lower molariform with a weaker cingulid. Differs from *G. haizhouensis* in being larger and having a weak cingulid on lower molariforms, a diastema between anterior teeth, and p1 more vertically implanted. Differs from *G. luoianus* (assuming its validity as a different species) in having one fewer upper molariform.

Remarks.—The original diagnosis of *G. zofiae* (Li et al. 2003) was considered not clear enough to distinguish it from other *Gobiconodon* species. Lopatin and Averianov (2015) noted that certain characteristics, such as p1 structure, dp2 root number, and the position of the posteriormost mental foramen, were identical in *G. zofiae* and *G. hopsoni*. Despite these similarities, *G. hopsoni* is notably larger than *G. zofiae*. For instance, the distal upper molariform (M5) of *G. hopsoni* measures 6 mm in length and 4.1 mm in width (Rougier et al. 2001), whereas the largest upper molariform of *G. zofiae* is only 2.6 mm by 1.86 mm. In adult individuals, as represented by the holotypes of both species, the size difference supports their distinction as separate species. Here, we use CT-scan rendered tooth morphologies of *G. zofiae* to further clarify its status as a valid species.

Lopatin and Averianov (2015) considered the holotype of *G. zofiae* (IVPP V12585) to represent an adult animal, corresponding to ontogenetic stage VI of *G. borissiaki*

(PIN 3101/9). This appears consistent with the wear on m3–5 of IVPP V12585, although the overall tooth wear is not completely clear due to damage to some tooth crowns. Nonetheless, all teeth appear erupted and functional, with the possible exception of dP3/dp3 in the adult stage. No tooth germs are present in the upper and lower jawbones. Additionally, IVPP V12585 has a double-rooted dp3, whereas the tooth at the same locus in PIN 3101/9 was single-rooted and interpreted as p2 (see Discussion below – this tooth could be a single-rooted p3 rather than a single-rooted dp3).

Material.—Type material only.

Description.—*Upper teeth*: The dental formula is revised as 2.1.3.4/2.1.3.5, although 2.1.3.4/3.1.2.5 is also possible (see Discussion). I1 is partially preserved and appeared larger than I2, as noted in the original study (Li et al. 2003). The alveolus of I1 is preserved and I2 is distinctly conical; both incisors are single-rooted. The upper canine is taller and mesiodistally longer than I2 and P1, transversely compressed and single-rooted. Although the premaxillary-maxillary suture is unclear, the morphology and position of this tooth suggest it is a canine rather than I3. Unfortunately, the tooth crowns of I2 and the canine were broken according to the CT images (Figs. 2, 3). In the original study, P1 was described as broken but interpreted as a small single-rooted tooth based on its alveolus. However, the CT-scan data revealed that there is no alveolus present, only a diastema distal to the canine (Fig. 2), indicating that the tooth identified as P1 in the original study does not exist. Consequently, P2 in the original study is redesignated as P1 in this study, followed by two premolariforms. P1 is single-rooted and smaller than I2, and has a crown lower than that of I2 with a blunt triangular shape in lateral view. P2 is double-rooted and the roots are even longer than those of the molariforms. The P2 crown is much larger than the P1 and as high as the M1. However, it is a typical premolariform in having a simple crown. The tooth has no cingulum. In the labial or lingual view, the tooth crown is predominantly formed by a large cusp A that is triangular with a gently convex anterior edge and a concave posterior edge, with a small cusp at the distal end of the crown.

The tooth distal to P2, identified as dP3, is double-rooted with much shorter and thinner roots compared to P2 and molariforms, suggesting that it was formed when the jawbone was thinner. The dP3 crown is notably smaller in all dimensions than those of P2 and molariforms. It is molariform, with three cusps, the central cusp A being the largest. The crown is deeply worn, with the worn tip of cusp A level with the cingulum of M1. Such a small and low tooth between the tall P2 and M1 appears non-functional in the adult dentition. The wear probably occurred when the animal was young. However, the CT scan reveal no tooth germ underneath the dP3, indicating that the dP3 will not be replaced by a successive tooth.

The molariforms show a lingual inclination that increases distally. The anterior end of the left M1 is fractured, with the portion bearing cusp B slightly shifted lingually (Fig. 2); if restored, cusps A, B and C would align mesiodistally. M1 is similar in length to M2 but narrower than other molariforms. Cusp A, the largest of the three main cusps, is less inflated compared to that of *G. gongzhulingensis*. The cingulum is well-developed and surrounds the crown. Cusps E and F are weakly developed at the mesiolingual and mesiolabial corners (Fig. 3), respectively. Cusps of M1 are less worn than those of M1–3, suggesting that it is a replacement tooth, probably M1R (Lopatin and Averianov 2015).

M2 has a pronounced labial cingulum that is decorated with minuscule cuspules. The cingulum labial to cusp C is convex labially in occlusal view. The main cusps are aligned mesiodistally. Cusp B is distinct but smaller than cusp C. The wear facet on cusp B faces mesiolingually, while that on cusp C faces distolingually.

M3 is the widest of the upper molariforms, with an expanded labial cingulum, particularly the portions labial to cusp B and C, forming an ectoflexus labial to cusp A. Several accessory cusps are present on the labial cingulum. The lingual cingulum is also expanded. The anterior portions of the lingual and labial cingula are wider than the posterior ones, making the anterior half of the tooth crown wider than the posterior half. The main cusps show an incipient triangular pattern (Kielan-Jaworowska and Dashzeveg 1998), with cusp A being slightly more lingual than cusp B and C. Cusp B is nearly erased by wear and the wear extends transversely across the anterior end of the crown, being deeper lingual to cusp B. The wear of cusp C is notable, facing distolingually. A wear facet is present at the distolingual corner of the crown. The general wear pattern is similar to that of *G. gongzhulingensis* (see below).

The mesiolabial portion of M4 is damaged, with the tooth appearing shorter than other molariforms, though three main cusps remain discernable. Its mesial half is as wide as the distal half of M3, while its distal half is narrower, resulting in a small cusp C. The wear at the mesiolingual end of the crown suggests M4 belongs to the same generation as M3. The roots of M4 are shorter than those of M3 and show a trend of fusion on the lingual side.

Lower teeth: We identify the mesial incisor as i1. The crown is broken, but the preserved portion shows an oval cross-section of the tooth base, with a long mesiodistal diameter of 1.9 mm and a short diameter of 1.2 mm. The root is long, extending posteroventrally to the level of the canine root ends, indicating an inclined but not procumbent tooth. The body of the root is flat on the lingual side and convex on the labial side.

The i2 is approximately half the thickness of i1 or less. Its crown is convex labially in both longitudinal and transverse directions, while the lingual side is concave in the longitudinal direction but convex in the transverse direction, with a bulging central region. The mesial and labial edges of the tooth are sharp.

The third tooth is morphologically similar to i2 but slightly lower, with the entire tooth (crown and root) shorter

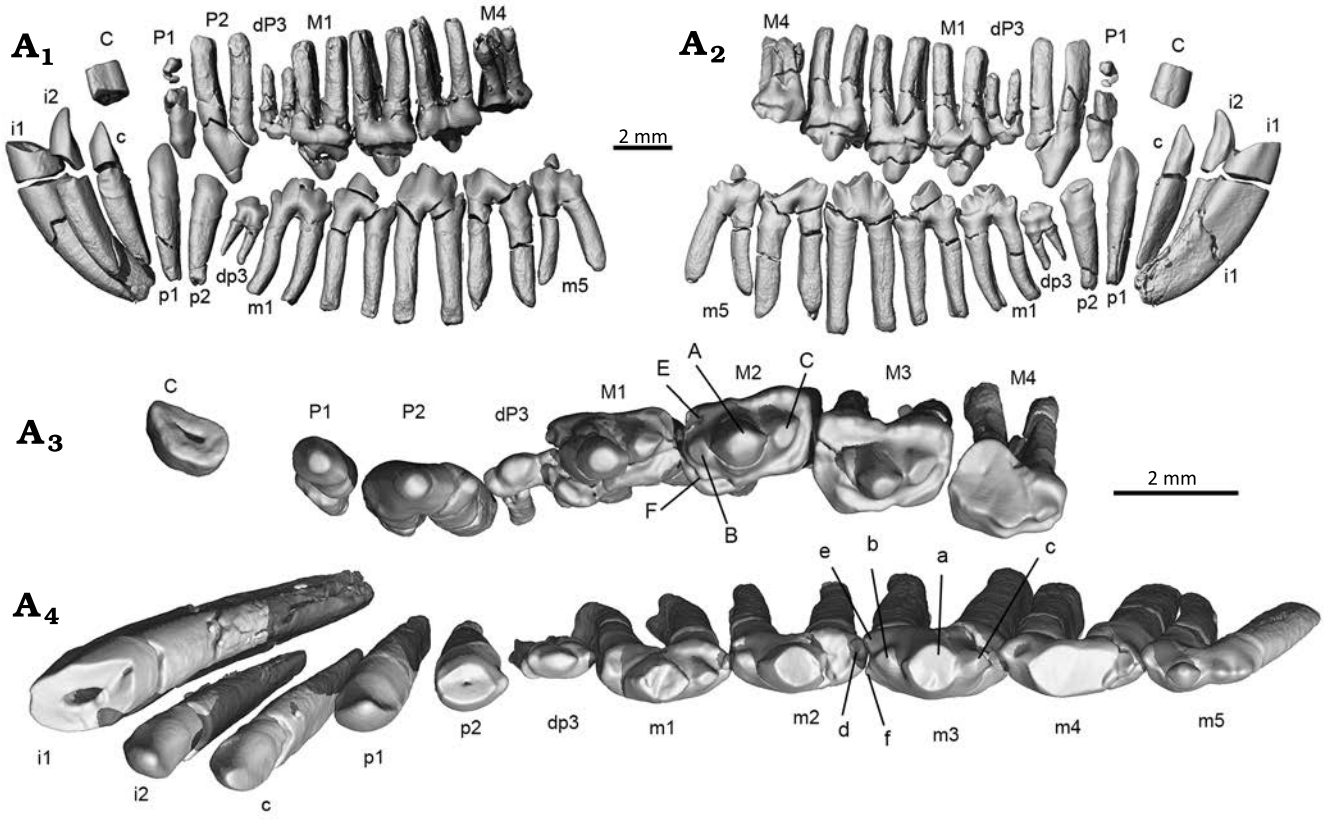

Fig. 3. CT-rendered images for the left dentitions of the gobiconodontid mammal *Gobiconodon zofiae* Li et al., 2003, holotype (IVPP V12585) from Lower Cretaceous of Lujiatun, Beipiao, China. Upper and lower dentitions in reconstructed occlusal position in lateral (A_1) and lingual (A_2) views. Upper (A_3) and lower (A_4) teeth in occlusal view.

than i2. When the upper and lower dentitions are aligned in the most possible occlusal positions (Fig. 3A_1, A_2), the third lower tooth is mesial or partly mesial to the upper canine. Based on its position, this tooth is identified as the canine, which is incisor-like and single-rooted.

The fourth tooth is also incisor-like, resembling the canine in shape and size. Thus, even if this tooth is identified as the canine, *Gobiconodon zofiae* would have a single-rooted and incisor-like lower canine. The tooth is separated from the canine by a diastema larger than that between i2 and the canine; it faces more lingually and is implanted more vertically than the canine. We identify this tooth as p1.

The crown tip of p2 is broken, but the preserved portion remains incisor-like, similar in size and morphology to p1. No lingual cingulid is present, but a distal bulge occurs at the base of the crown. The p2 is vertically implanted. A ring-shaped ridge encircles the proximal portion of the root, marking the edge of the alveolus. For convenience of description, we term this ridge as the alveolus ridge. The root below the alveolus ridge, implanted in the jawbone in life, has a rough surface, whereas the root section above the alveolus ridge but below the crown is smooth and lacks enamel. The alveolus ridge is present in nearly all teeth, but more distinct in the lower ones. A similar condition is probably present in other species of *Gobiconodon* (Jenkins and Schaff 1988; Kielan-Jaworowska and Dashzeveg 1998; Lopatin and Averianov 2015; Kusuhashi et al. 2016).

The tooth distal to p2 is identified as dp3, corresponding to its upper counterpart. As in other *Gobiconodon* species, dp3 (or its successor) is the smallest postcanine tooth. The dp3 is double-rooted, with root thickness and length less than half those of p2 and m1. Although small, it is molariform, bearing three cusps with cusp a being the largest. The tooth crown is as long as p2 but approximately half its width. Cusp a is positioned slightly anteriorly on the crown and cusp c is larger than cusp b. All the cusps are worn and the crown is lower than cusp b of m1. There is no cingulid on the lingual side of the crown. The alveolus ridge is distinct, with the proximal portions of the two roots fused above it. Similar to its upper counterpart, this small, low tooth between the tall p2 and m1 is likely functional only in juvenile stages.

Five lower molariforms share a similar general shape. The tips of cusp a on various teeth in both left and right dentitions are broken, but cusp a remains discernable as tilting slightly distally. No cingulid is present on the labial side of the crown, but a poorly developed cingulid is observed on the lingual side, most distinct on the lingual side of cusp c. Cusp a of m1 is positioned mesially. Cusp c is larger and

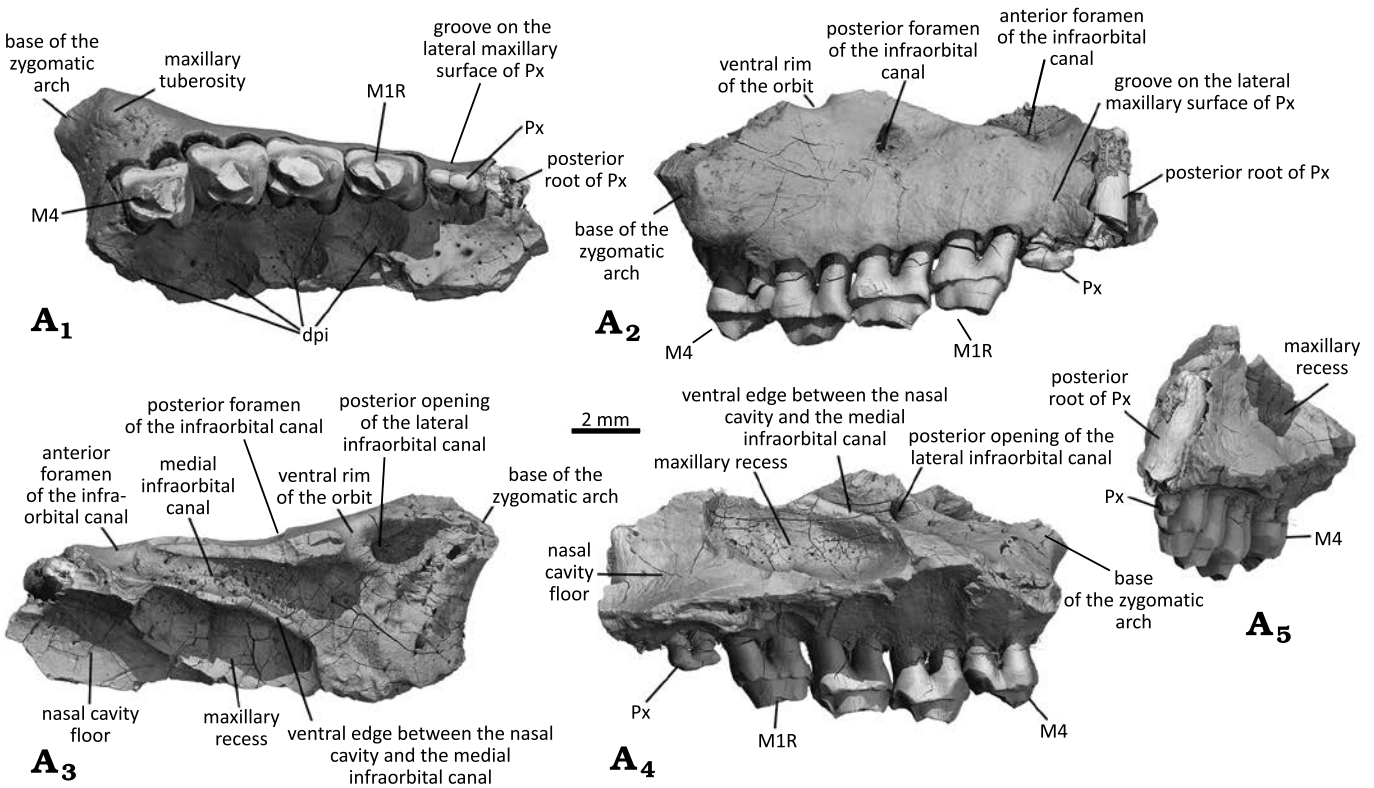

Fig. 4. Right maxilla with dentition of the gobiconodontid mammal *Gobiconodon gongzhulingensis* sp. nov., holotype (RCPS VJ8001) from Late Cretaceous of Shanqian, Gongzhuling, China. Maxilla fragment and upper cheek teeth (ultimate premolariform and M1–2R, M3–4) in ventral (A_1), lateral (A_2), dorsal (A_3), medial (A_4), and anterior (A_5) views.

positioned higher than cusp b. A wear facet is present on the labial side of cusp c, and a small cusp d is located at the distal base of cusp c. The tiny cusp e is situated lingual to cusp b. Cusp f is absent in m1. The m2 is larger and taller than m1 with all cusps slightly larger than in m1, and cusp e becoming more distinct. A small wear facet is present on the mesiolabial side of cusp a. The m3 is larger than m2, with a distinct cusp e and a small cusp f; both forming a notch at the anterior end of the crown that interlocks with cusp d of m1. Although cusp f is indiscernible on most lower molariforms, an interlocking pattern appears to exist between adjacent lower molariforms. The m4 is similar to m3 in shape and size, with a distinct cusp e and a reduced cusp f. Cusp c is pronounced in m3–4, separated from cusp a by a notch. The m3 and m4 exhibit the deepest wear among the lower molariform, with a large, flat wear facet primarily on cusp a and b, extending to the base of the crown and facing mesiolabially. At the deepest wear area, the enamel is worn away, exposing light-colored dentine. The m5 is the smallest of the lower molariforms, with a proportionally small cusp a and a low cusp c, separated from cusp a by a distinct notch. Due to its reduced size, the wear facet is relatively small, and primarily on the lateral side of cusp b and its base. Based on the wear patterns, m3–m5 likely belong to the same tooth generation, while m1 and m2 are from a younger generation.

Stratigraphic and geographic range.—Type locality and horizon only.

Gobiconodon gongzhulingensis sp. nov.

Figs. 4–6.

Zoobank LSID: urn:lsid:zoobank.org:act:006164BE-8715-4C70-A792-B02152E8A905

Etymology: Referring to the city Gongzhuling, Jilin Province, where the type locality is located.

Holotype: RCPS VJ8001, a partial right maxilla with dP3, M1–2R, M3–4, and the root of P2 (Fig. 4).

Type locality: Shanqian Village, Liufangzi Town, Gongzhuling City, Changchun Area, Jilin Province, northeast China.

Type horizon: Quantou Formation, lower Upper Cretaceous, Cenomanian to middle Turonian, (Wan et al. 2013; Xi et al. 2019; Wang et al. 2016, 2022b). The age determination of the Quantou Formation to the Cenomanian to middle Turonian is based on the work by Wan et al. (2013), Xi et al. (2019), and Wang et al. (2016, 2022b). Given this age, *Gobiconodon gongzhulingensis* would date from the early Late Cretaceous, representing one of the youngest species of Gobiconodontidae. However, Wang et al. (2009) hold the view that the Quantou Formation is Albian. In the study on the zalambdalestid *Zhangolestes jilinensis*, Zan et al. (2006) reviewed the various views about the age of the Quantou Formation and chose the age: "Cretaceous, most probably early Late Cretaceous" (Zan et al. 2006: 155). Given that the zalambdalestids, such as the basal zalambdalestid *Kulbeckia kulbecke* (Archibald and Averianov 2003), came from the Late Cretaceous (Coniacian), the early Late Cretaceous age of the Quantou Formation appears to be consistent with the general temporal distribution of zalambdalestids.

Material.—Type material only.

Diagnosis.—Upper tooth row increases in height from M1R

to M3 with a step-like cingulum alignment and end-to-neck upper tooth contact; cusp A inflated and cusp B lost in M1R and M4; cusps A, B, and C show a weak triangulation in arrangement; the width to length ratio of M3 0.77; a strong and singled rooted P2. The base of the zygomatic process of the maxillary is posterior to M4.

Remarks.—G. gongzhulingensis further differs from *G. borissiaki* in having a stronger single-rooted P2 and a more reduced dP3 (in our interpretation, but M1 in others); differs from *G. hoburensis* in having a double-rooted dp3 (dp2 in others; Lopatin and Averianov 2015: figs. 13, 14; note that this tooth was labeled as p2); differs from *G. ostromi* and *G. hopsoni* in being smaller and upper molariforms with wider cingulum; differs from *G. palaios* and *G. bathoniensis* in having a more rectangular outline of the upper molariforms; differs from *G. luoianus* in having four instead of five upper molariforms. It is impossible to compare *G. gongzhulingensis* with *G. tomidai* and *G. haizhouensis* which have only lower teeth preserved, but the correlation of the upper and lower teeth in other species suggests that the upper molariforms of *G. tomidai* and *G. haizhouensis* would not be as wide as those of *G. gongzhulingensis.* It is similar to *G. zofiae* in having a reduced ultimate premolariform and four molariforms, but differs in having the ultimate upper premolariform and M4 less reduced and in having cusp A of the molariforms more inflated and cusp B and C proportionally small; cusp B is absent in M1R and M4; the penultimate premolariform is much stronger. See Table 1 for tooth measurements.

Description.—Maxilla: *Gobiconodon gongzhulingensis* is represented by a partial right maxilla bearing the presumed root of the penultimate premolariform (P2), the ultimate deciduous premolariform (dP3), and four molariforms (M1–2R, M3–4) (Fig. 4). The preserved portion of the maxilla appears undistorted. In ventral view, the bony palate preserves partial palatal process of the maxilla with a small posterior portion possibly from the palatine. The zygomatic process of the maxilla is robust, projecting posterolaterally from the region containing the ultimate molariform (M4). The posterior root of M4 is slightly anterior to the anterior root of the zygomatic arch. There is a thin wall of bone that posteriorly closes the alveolus of M4, indicating that there is no space for additional tooth germ; the CT-scan image also confirms this (Fig. 5). Thus, we interpret this specimen as belonging to an adult individual, older than those with tooth germs or replacement (e.g., Jenkins and Schaff 1998; Lopatin and Averianov 2015; Lopatin 2022). A blunt swelling, the maxillary tuberosity, is present at the zygomatic base. On the medial side of the tooth row, there exist four dental pits, of which three distinct and deep ones are medial to M1–2R, and M3, respectively, and a shallow and incomplete one is medial to M4. These pits are presumably to accommodate tall and conical cusps, at least cusp a, of the lower molariforms when the lower jaw is in a resting position. There is no pit medial to dP3, suggesting that there

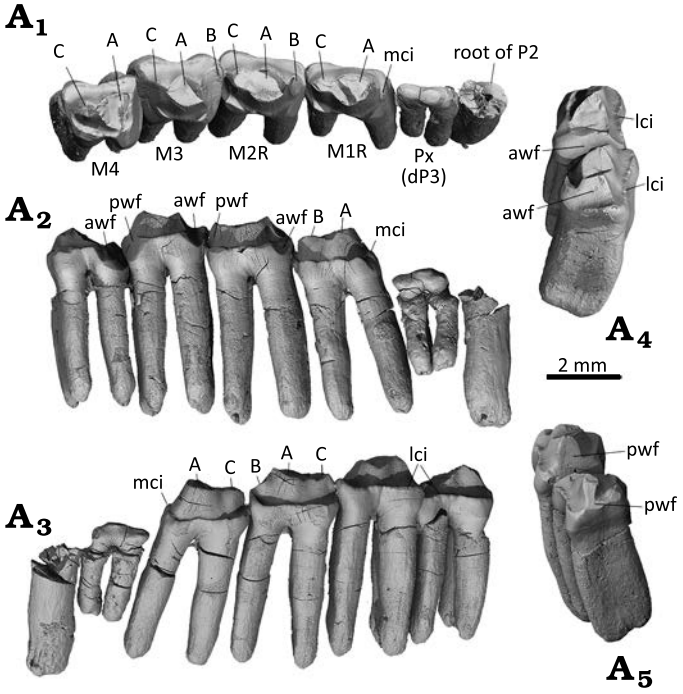

Fig. 5. Dentition of the gobiconodontid mammal *Gobiconodon gongzhulingensis* sp. nov., holotype (RCPS VJ8001) from Upper Cretaceous of Shanqian, Gongzhuling, China. Right upper postcanines in occlusal (A_1), lingual (A_2), and labial (A_3) views; right M3–4 in mesial (A_4) and distal (A_5) views. Abbreviations: awf, anterior wear facet; lci, labial cingulum; mci, mesial cingulum; pwf, posterior wear facet.

is no tall cusp of the corresponding lower tooth, either m1 or the ultimate premolariform, a condition similar to that of *Gobiconodon zofiae* (IVPP V12585; Fig. 2). The region containing the small dP3 exhibits a gentle concavity or "necking" between the alveoli of M1R and the penultimate premolariform P2. This cranial configuration corresponds to the fact that dP3 is small, both crown and roots, compared to those of P2 and M1R. Additionally, numerous tiny nutrient foramina are scattered across the bone surface.

In lateral view, only the basal portion of the facial process of the maxilla is preserved, showing a dorsomedial extension in anterior view. No buccinator ridge is present (see Rougier et al. 2001). The most conspicuous feature is the orifice above M2R, which is the posterior foramen of the infraorbital canal; its posterior opening is revealed in the dorsal and medial views of the fragmentary maxilla. Dorsal to dP3, the surface of the maxilla displays a vertical and shallow groove between the areas containing M1R and P2, due to the small size of dP3 as noted above. If the bony wall for the dP3

Table 1. Tooth measurements (in mm) of *Gobiconodon gongzhulingensis* sp. nov.

Tooth	dP3	M1R	M2R	M3	M4
Length	1.53	2.22	2.45	2.43	2.17
Width	0.63	1.32	1.61	1.87	1.93
Width to length ratio	0.41	0.59	0.66	0.77	0.89

alveolus were intact, this grooved configuration would be more clearly shown. This feature is absent in other species of *Gobiconodon* (Kielan-Jaworowska and Dashzeveg 1998; Lopatin and Averianov 2015; Li et al. 2003; Fig. 2).

The broken dorsal margin of the facial process does not represent the natural edge of the suture with the nasal. Two features are notable along this margin. The first is a concave notch posterodorsal to the infraorbital foramen. The rim of the notch is smooth; in dorsal view, it continues as a smooth surface anterodorsal to the posterior opening of the infraorbital canal and merges with the maxillary platform that forms the ventral floor of the orbital socket. This notch likely forms part of the anteroventral rim of the orbit. If true, this configuration indicates that the orbital rim is somewhat indented at its anteroventral corner. The second feature is a notch anteriorly confluent with the vertical groove above dP3. This notch forms the ventral rim of another foramen of the infraorbital canal, which is larger than the posterior one. In dorsal view, the canal is visible and extends posteriorly to the maxillary platform (see below). Thus, *G. gongzhulingensis* has two foramina of the infraorbital canal, with the anterior one being larger. This is similar to other species with this region preserved, such as *G. hoburensis* (PIN 3101/21; Trofimov 1978), *G. borissiaki* (PIN 3101/19; Lopatin and Averianov 2015), and *G. hopsoni* (PSS-MAE 140; Rougier et al. 2001).

In dorsal and medial views, the maxilla forms a platform or shelf on the anterior floor of the orbit (the orbital platform). The floor is posteriorly demarcated by a gently curved edge, and is uneven, with a single root tip (M3 by position-check) visible. On the lateral side, there is the posterior opening of the posterior infraorbital foramen, which is fully separated from the posterior opening of the canal that ends as the anterior infraorbital foramen. This suggests the presence of two separate canals, a short lateral one and a longer medial one. The external infraorbital canal is relatively short, about half the length of the medial canal. The medial infraorbital canal, as indicated by its larger anterior opening, is broad and gradually widens into the orbital floor, visible due to the broken bone roofing the canal. The canal lies generally above and parallel to the tooth row. On the floor of the canal, as well as that of the orbit, there are many miniscule foramina; these foramina show a trend of opening posteriorly or posteromedially and each is followed by a short groove on the floor. Medially, the canal is walled by a bony plate that separates the canal from the nasal cavity. However, a smooth section along the posterior part of this wall, best observed in medial view, indicates a broad opening that, if not covered by soft tissue in life, connects the posterior part of the medial infraorbital canal to the nasal cavity. Medially, an oval pocket, identified as the maxillary recess based on its shape and position, occupies the posterolateral floor of the nasal cavity, as in mammaliaformes morganucodontan *Cifellilestes cisco-ensis* (Davis et al. 2022: fig. 4), comparable to the maxillary sinus in *Morganucodon watsoni* (Kermack et al. 1981: figs. 13, 14). The maxillary recess is medially bounded by raised thin bone. However, this structure has not been reported in eutriconodonts yet. The floor of the recess is generally smooth, except for numerous small foramina. Anteromedial to the recess is a flat surface of the bone, which is the floor of the nasal cavity and the dorsal surface of the palate or the palatal shelf as described by Kermack et al. (1981). No evidence of nasal turbinals is observed in these regions.

Dentition: A tooth root is preserved at the anterior end of the preserved maxilla, interpreted as belonging to a single-rooted P2. Although the crown is broken and the anterior part of the maxilla is missing, two reasons support this interpretation. First, the root is thick, exceeding the thickness of molariform roots. If it were the posterior root of a double-rooted tooth, the anterior root would likely be even thicker, as the main cusp of p2 is commonly mesially positioned to withstand greater stress, as observed in *G. zofiae* (Fig. 2). Such a tooth would be unusually large (e.g., larger than P2 of *G. zofiae*), which is uncommon or unknown in any species of *Gobiconodon* with known upper dentitions. Second, the cross-section of the root is circular. For a double-rooted tooth, the two roots usually show antero-posterior compression. A single-rooted P1 and P2 are present in the paratype of *G. borissiaki* (PIN 3101/19), but P2 is double-rooted in *G. hoburensis* (Trofimov 1978; Lopatin and Averianov 2015) and *G. zofiae* (Li et al. 2003; Fig. 2).

Five postcanines are preserved, identified as dP3, M1R, M2R, M3, and M4 based on their shape, size, and degree of wear. As in *Gobiconodon zofiae*, dP3 is molariform in having cusp A, a slightly smaller cusp C, and a very small cusp b, but is notably small and narrow. The crown is also positioned considerably lower than M1R, as in *G. zofiae*. The crown's appearance is influenced by wear, lacking a cingulum. The two roots are much thinner and shorter than those of P2 and molariforms, but relatively thick or inflated for such a small crown. This morphology suggests that dP3 is a deciduous tooth, or the oldest tooth generation in the tooth row, formed when the dentary was shallow during early ontogeny, as observed in *G. zofiae*. The low position of the worn dP3 between P2 and M1R indicates it was functional before other teeth erupted but had little function in adulthood. As in *G. zofiae* and *G. gongzhulingensis*, dP3 and dp3 are not widened.

The upper molariforms may have a slight lingual inclination, although this inclination is minimal when compared to *Gobiconodon hoburensis*, where a 60° angle is formed between the palatal process and vertical axis of the dentition (Lopatin and Averianov 2015). Each molariform possesses two long roots, anteroposteriorly compressed and tapering distally to a rounded end. Although the tips of the molariforms are broken, cusp sizes and crown morphologies remain discernible.

The M1R crown has a rectangular outline in occlusal view, with a narrow transverse width-to-length ratio of 0.59 (see measurements in Table 1). Cusp A is predominant and inflated, merging with cusp C at its base. These two cusps are separated by a very shallow groove on both lingual and

labial sides. At the anterior end of the crown there is an anterior cingulum, part of which shows a slight widening but does not form a cusp. Cusp B is absent. In lingual view, the lingual cingulum is developed, with a narrow median gap in the occlusal view. The lingual cingulum is formed by four small cuspules, with the mesial and distal ones being stronger, forming a shelf-like corner in occlusal view. The mesial corner has been partly erased as shown by an inclined wear facet that faces mesiolingually, whereas the distal corner is truncated by a narrow wear facet that extends to the distal end of the tooth crown. The labial cingulum is complete in labial view, with a narrow middle portion. The distal end of the cingulum expands to form a lobe at the distolabial corner of the crown.

From M1R to M4, a general trend is the proportional widening of the crown so that the molariforms become more square-shaped posteriorly. M2R is essentially a transversely widened version of M1R, reflected by its wider cusps, cingula, and roots. The width-length ratio is 0.66. However, M2R differs from M1R in having a small cusp B. The wear facet that nearly erased cusp B is confluent with the one on the mesiolingual corner of the crown, similar to that of M1R but more pronounced. Cusp A is inflated but its tip is broken. Cusp C is larger than cusp B. The three main cusps do not show triangulation, differing from those in other species (e.g., Kielan-Jaworowska and Dashzeveg 1998).

M3 has a width-length ratio of 0.77. Its further widened mesiolabial corner results in a two-lobed labial cingulum separated by a median ectoflexus. Cusp B was probably present in life, based on the space mesial to cusp A, but it would be small and has been completely worn away. An extensive wear facet (anterior wear facet) gouges transversely along the anterior tooth crown. This wear also erased the anterior part of cusp A. A similarly extensive wear facet (posterior wear facet) exists on the distolingual corner of the crown; this facet nearly erases cusp C.

M4 is slightly lingual to M3 and smaller, with a width-length ratio of 0.89. Anteriorly, there is a large anterior wear facet that extends the full width of the tooth crown except for the very mesiolabial corner. This wear facet is most extensive at the mesiolingual corner of the crown, forming an inclined facet facing mesiolingually and cutting part of cusp A. If cusp A is conical, the space mesial to it would be too narrow to bear cusp B; thus, we interpret that M4 lacks cusp B. The wear facet on the distal side of the crown indicates that there must be a lower molariform (m5) that is at least partly distal to M4 and worked against it; thus, it can be inferred that, as in G. *zofiae*, there should be five lower molariforms in the lower dentition.

In lingual or labial view of the upper dentition, M3 is positioned highest in the molariform row. The distal end of M2R fits into the concave area, the neck or cervical region, at the crown-root transition on the mesial end of M3. Similarly, M1R has the same end-to-neck relationship with M2, but at a lower position in the dentition. This results in a gradual decrease in height from M3 to M1R, with the cingula of the teeth forming a step-like alignment from highest to lowest. In contrast, the mesial end of M4 fits into the cervical region of M3 on its distal side. Other species like *Gobiconodon hoburensis* (PIN 3101/40; Lopatin and Averianov 2015) and *G. zofiae* (Li et al. 2003; Fig. 2) do not have this end-to-neck tooth contact pattern. Instead, their molariforms show an end-to-end contact and the cingula are aligned at a similar level. In *G. zofiae*, the tooth height decreases from M1R to M4 in the opposite direction compared to *G. gongzhulingensis*. A similar trend is observed in *Gobiconodon hoburensis*, though less pronounced than in *G. zofiae*. It is possible that the end-to-neck tooth contact in *G. gongzhulingensis* may represent a distinct type of tooth interlocking mechanism or, alternatively, a transitional configuration associated with successive generations of tooth eruption.

Tooth wear: Tooth wear has been used as an indicator for identifying tooth generation in *Gobiconodon* (Lopatin and Averianov 2015) and for interpreting occlusal patterns in triconodontids more broadly (Jäger et al. 2020). In *Gobiconodon gongzhulingensis*, the dP3 is heavily worn, with wear concentrated on the apices of the cusps, resulting in a markedly flattened crown. SEM observations show that the wear facets are slightly convex and irregular in outline, lack sharp marginal edges, and appear polished, bearing either no striations or only faint ones. Such wear characteristics are consistent with abrasion-dominated processes (Koenigswald et al. 2013; Ungar 2015). Because direct tooth-to-tooth contact appears unlikely for dP3, given its substantially lower position relative to P2 and M1R in the adult dentition, the observed wear is unlikely to reflect active occlusal shearing. Instead, the wear pattern may reflect abrasion associated with the consumption of relatively soft food during an earlier ontogenetic stage, subsequent modification by non-occlusal abrasion later in life, or a combination of both processes. In *Gobiconodon*, the premolars are labiolingually more compressed and generally smaller than the molariforms, suggesting a primary role in holding or dividing food rather than in active mastication. Accordingly, regardless of the specific mechanism involved, the wear observed on dP3 does not provide evidence for a shearing function.

The wear facets are well-preserved on the molariforms of *G. gongzhulingensis* (Fig. 6). M3 and M4 exhibit the most extensive wear facets, with wear decreasing toward M1R. M2R shows deeper wear than M1R but less than M3–4. Heavier wear of the molariforms M3–4 than M2 in *G. borissiaki* was considered indirect evidence of molariform replacement (Kielan-Jaworowska and Dashzeveg 1998). However, wear intensity in taxa exhibiting embrasure shearing occlusion may be strongly influenced by functional factors and does not necessarily correlate directly with relative tooth age or eruption timing. Accordingly, we refrain from using differential wear alone as a definitive indicator of eruption sequence. Instead, the observed pattern is more conservatively interpreted as being consistent with the possibility that

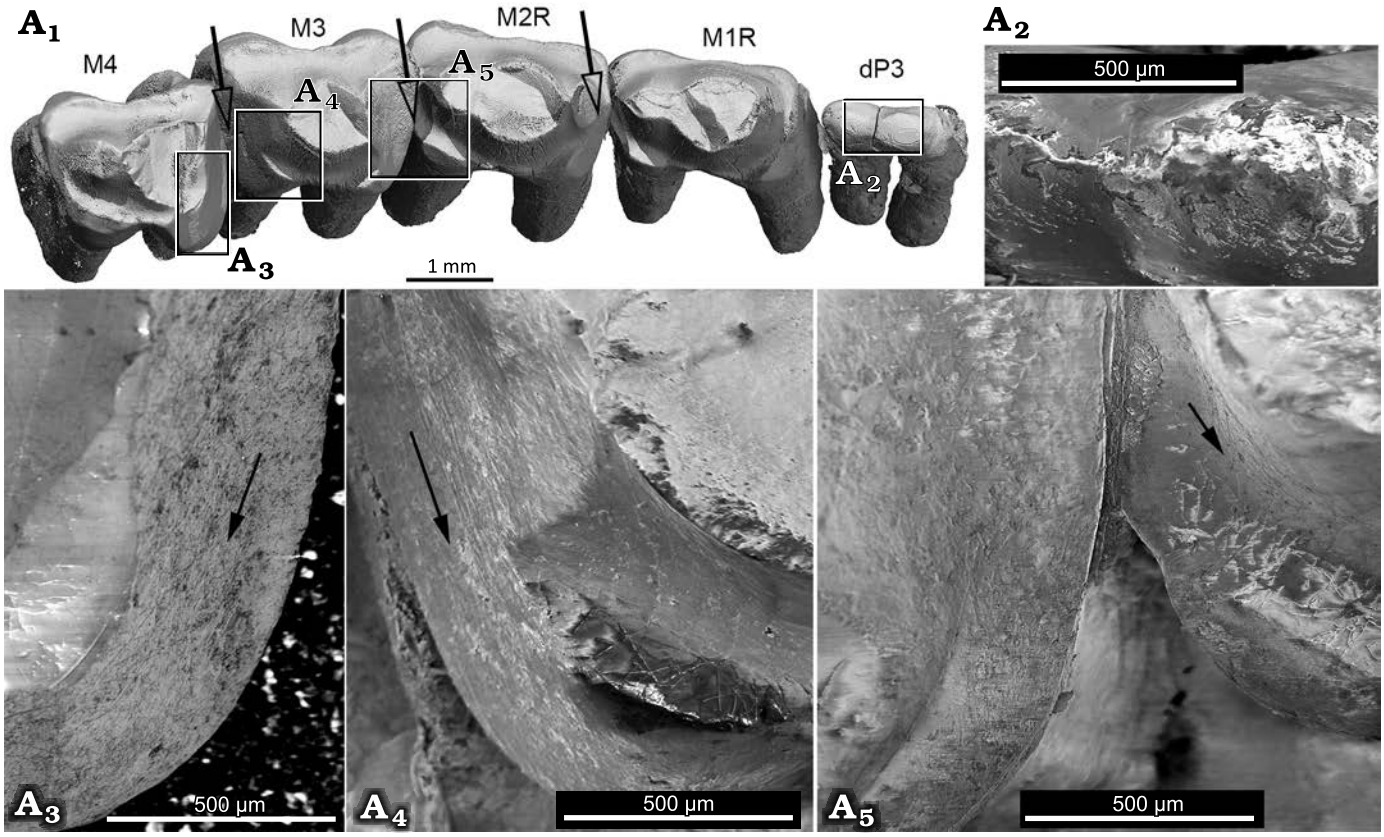

Fig. 6. Tooth wear of the gobiconodontid mammal *Gobiconodon gongzhulingensis* sp. nov., holotype (RCPS VJ 8001) from Upper Cretaceous of Shanqian, Gongzhuling, China. dP3–M4 in occlusal view, the white arrows indicate the moving directions of the lower teeth (A_1); close-up views (A_2–A_5), black arrows indicate the general directions of the striations on the enamel. There is a weak sign of striations on the deeply worn area of the mesial wear of M3 where the dentine is exposed (left tooth in A_5).

M3–4 belong to an earlier functional cohort than M1–2R, with M2R potentially entering occlusion before M1R.

The wear pattern of the molariforms indicates embrasure occlusion in which wear facets are primarily on the mesial and distal sides of the teeth. The striations on the teeth are perpendicular to the vertical axis or the roots, indicating a labiolingually directed component of relative movement between the lower and upper dentitions during occlusion. Cusp a of the lower molariforms gauged the embrasure between two adjacent upper molariforms to create a groove on the tooth crown, similar to that of *Gobiconodon borissiaki* (Kielan-Jaworowska and Dashzeveg 1998). Wear facets vary in size depending on the degree of wear. Generally, the wear facets are flat with clear marginal edges separating them from the surrounding enamel and bear distinct striations with major directions; this is typical of tooth attrition (Koenigswald et al. 2013). The deepest wear occurs on the mesial sides of M3–4 and the distal surface of M3. This differs from *G. borissiaki* (PSS 10-15b, Kielan-Jaworowska and Dashzeveg 1998: fig. 1A–C), where the wear groove is primarily along the distal end of the mesial tooth. These differences suggest distinct occlusal positions of cusp a of the lower molariform against the upper molariforms in the two species. At the mesial end of M3, the enamel is worn away, exposing dentine without preserved striations (Fig. $6A_4$). Toward the lingual margin of the crown, the wear surface grades from a subhorizontal facet into a steeper, inclined facet that extends toward the crown base. The wear facets on the dentition of *G. gongzhulingensis* indicate an embrasure occlusion and strong labiolingual movement of cusp a of the lower teeth and mandible, similar to *G. ostromi* (Jenkins and Schaff 1988) and *G. hoburensis* (Kielan-Jaworowska and Dashzeveg 1998), broadly comparable to the occlusal patterns reported observed in *Priacodon* (Jäger et al. 2020) and *Dryolestes* (Schultz and Martin 2014).

Stratigraphic and geographic range.—Type horizon and locality only.

Discussion

Tooth formula of *Gobiconodon*.—In the original study (Li et al. 2003), the tooth formula of *Gobiconodon zofiae* was reported as 2.1.4.4/1.1.4.5. This lower tooth formula was widely recognized for *Gobiconodon* at the time (Jenkins and Schaff 1988; Kielan-Jaworowska and Dashzeveg 1998; Maschenko and Lopatin 1998; Kielan-Jaworowska et al. 2004). It was heavily influenced by *Gobiconodon ostromi*, which has well-preserved lower dentitions and a known

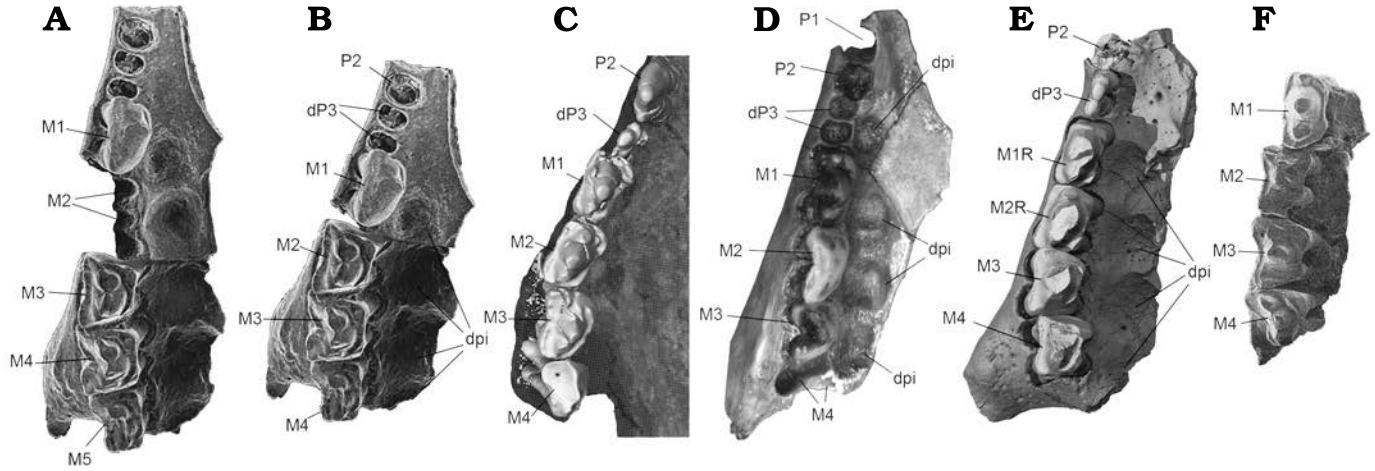

Fig. 7. Comparative upper right tooth row in occlusal view of *Gobiconodon* species. **A**. Original interpretation of the upper molariforms of *Gobiconodon hoburensis* Trofimov, 1978 (Upper Cretaceous of Khoboor locality, Guchin Us Soinon, Gobi Desert, Mongolia), based on a composite of two maxilla fragments with teeth (PSS 1047a and lG-37b; Kielan-Jaworowska and Dashzeveg 1998: fig. 5) where five molariforms were reconstructed. **B**. Reinterpretation of the upper molariforms of *G. hoburensis* where there are four molariforms. **C**. The upper postcanines of *Gobiconodon zofiae* Li et al., 2003 (holotype IVPP V12585; Lower Cretaceous of Lujiatun, Beipiao, China); for comparison. **D**. Reinterpretation of the upper molariforms of *Gobiconodon borissiaki* Trofimov, 1978, (PIN 3101/19; Upper Cretaceous of Khoboor locality, Guchin Us Soinon, Gobi Desert, Mongolia, after Lopatin and Averianov 2015: fig. 12b). **E**. The upper postcanines of *G. gongzhulingensis* sp. nov. **F**. Reinterpretation of the upper molariforms of *G. borissiaki* (PSS 10-15b; Kielan-Jaworowska and Dashzeveg 1998: fig. 1A;). Abbreviations: dpi, dental pits. Not to scale.

ontogenetic sequence (Jenkins and Schaff 1988). However, the upper dentition of *G. ostromi* is only partially preserved.

Based on specimens assigned to *Repenomamus* and *Meemannodon* (Li et al. 2001; Wang et al. 2001; Meng et al. 2003, 2005; Hu et al. 2005), Meng et al. (2005) identified the upper canine by its position relative to the premaxillary-maxillary suture, with the lower canine mesial to its upper counterpart, as proposed by others (Clemens and Lillegraven 1986; Butler and Clemens 2001). The dental formula was thus identified as 3.1.2-3.4/2.1.2-3.4 in *Repenomamus* and considered applicable to gobiconodontids. An alternative dental formula of 2.1.2-3.5 for gobiconodontids was also suggested (Meng et al. 2005). Rougier et al. (2007) argued that a lower dental formula of 3.1.2.5 for *Gobiconodon ostromi* is equally defensible or preferable based on tooth shape. The lower dental formula of 3.1.2.5 for *Gobiconodon* is adopted by Lopatin and Averianov (2015), whereas that of 2.1.2-3.5 was recognized by Kusuhashi et al. (2016).

As described above, the P1 in the original study does not exist, resulting in a total of ten upper teeth. Although the premaxillary-maxillary suture is unclear in the holotype skull of *Gobiconodon zofiae*, the upper canine inferred by its size, morphology, and position appears convincing (Fig. 2). Thus, we recognize the upper dental formula of *G. zofiae* as 2.1.3.4. For the lower dentition, the three teeth distal to the enlarged i1 are similar in size and shape, making it difficult to identify the canine based solely on these traits. However, *Gobiconodon* is known to have embrasure occlusion (Jenkins and Schaff 1988; Kielan-Jaworowska and Dashzeveg 1998), allowing reconstruction of the occlusal relationship of the upper and lower dentitions of *G. zofiae* (Fig. 3A_1, A_2). This reconstruction is further supported by tooth wear patterns. For example, the mesiolabial surface of m5 bears a wear facet, but there is no wear on its distal half, indicating that the distal upper molariform (M4) occludes between m4 and m5. This suggests a general occlusal pattern where a lower tooth, such as m1, is approximately half a tooth mesial to its upper counterpart (M1), which is the general rule for mammalian occlusion. Based on this occlusal relationship and the identification of the upper canine, the third lower tooth is designated as the lower canine, resulting in a lower dental formula for *G. zofiae* of 2.1.3.5, which can be generalized as 2.1.2-3.5 for *Gobiconodon*.

Another feature of *Gobiconodon* is that the ultimate premolariform is the smallest postcanine, at least in the lower dentition (Jenkins and Schaff 1988). This appears applicable to both upper and lower dentitions, as evidenced by the holotype of *G. zofiae*. For incomplete dentition, this smallest tooth can serve as a reference for tooth assignment. Specimens with only two lower premolariforms likely reflect the shedding of the small dp3.

The upper dental formula of *Gobiconodon* remains uncertain due to the rarity of specimens preserving the upper dentition. In *G. ostromi*, two upper molariforms are preserved, interpreted for descriptive purposes, as M3 and M5, though the total number of molariforms is uncertain (Jenkins and Schaff 1988). The presence of five upper molariforms in *Gobiconodon* was further advocated by Kielan-Jaworowska and Dashzeveg (1998: fig. 5), and Lopatin and Averianov (2015), based on a composite dentition from two fragmentary specimens assigned to *G. hoburensis*. Compared to the upper dentitions of *G. zofiae* and *G. gongzhulingensis*, an alternative reconstruction of the upper molariform series of *G. hoburensis* is proposed (Fig. 7). In the reconstructed upper molariform series of *G. hoburensis* (Kielan-Jaworowska

and Dashzeveg 1998: fig. 5), the smallest tooth, indicated by its alveoli, is likely the ultimate premolariform, or dP3, as in *G. zofiae*. Distal to this tooth there are five molariforms and five dental pits located medially. This reconstructed series, along with the rostrum and palate, appears unusually long. Compared to the upper dentition of *G. zofiae*, the alternative reconstruction is shown in Fig. 7C in which the first tooth preserved in the posterior part of the fragmentary maxilla can be interpreted as M2 instead of M3. This new reconstruction makes more sense in the general morphologies of the tooth row and the rostrum as well as their occlusal relationship with the five lower molariforms. In addition, the reconstructed maxilla, at least the anterior part of *G. hoburensis* (PSS 10 37a; Kielan-Jaworowska and Dashzeveg 1998; Fig. 7) resembles the paratype maxilla of *G. borissiaki* more than other specimens assigned to *G. hoburensis* (PIN 3101/19; Trofimov 1978; Lopatin and Averianov 2015: fig. 12). This is because the alveolus size of the ultimate premolariform (or deciduous premolariform) is similarly small in the two specimens, whereas the alveolus mesial to it is notably larger and circular in PSS 10 37a, which is probably for a single-rooted tooth, as in PIN 3101/19. These size variations are less pronounced in the upper tooth row of other *G. hoburensis* specimens.

The tooth count, morphology and wear patterns of *G. zofiae* indicate that the upper molariform would occlude between two lower molariforms, known as embrasure occlusion (Jenkins and Schaff 1988; Kielan-Jaworowska and Dashzeveg 1998), in which the upper molariform is a half-tooth distal to its corresponding lower counterpart (Kusuhashi et al. 2016). For instance, M1 occludes between m1 and m2, a half-tooth distal to m1. Based on the dentition of *G. zofiae*, it is likely that all species of *Gobiconodon* have one upper molariform less than lower molariforms, suggesting that *Gobiconodon* has four upper molariforms rather than five (Kusuhashi et al. 2016). This hypothesis is supported by *G. gongzhulingensis*, indicating a general pattern that the upper molariform count is one tooth fewer than the lower ones in eutriconodontans. For instance, three upper and four lower molariforms are present in *Priacodon fruitaensis* (LACM 120451; Jäger et al. 2020).

Notably, *Gobiconodon luoianus* was originally described based on a skull (HGM41H III-0320) with associated dentaries, interpreted as having a dental formula of 2.1.2-3.5/2.1.3.5 (Yuan et al. 2009). Conversely, *G. zofiae* was originally interpreted as having four upper molariforms (Li et al. 2003), differing from the five-upper-molariform condition in *G. luoianus*. However, Lopatin and Averianov (2015) reinterpreted the lower dental formula of *G. luoianus* as 3.1.2.5 and considered *G. luoianus* as the junior subjective synonym of *G. zofiae*. They did not address the upper dental formula of *G. luoianus*. As the dentition of *G. luoianus* was only visible laterally (Yuan et al. 2009: fig. 2), the four-upper-molariform condition in *G. luoianus* cannot be ruled out. Additionally, given its preservation, *G. luoianus* may have had six lower molariforms (Kusuhashi et al. 2016) with the ultimate lower one often small and vestigial (Martin and Schultz 2023).

Tooth occlusion, tooth widening and diet of *Gobiconodon*.—The triconodontid tooth pattern is characterized by having three main cusps aligned mesiodistally in a row, usually with the central cusp (A in the upper and a in the lower) being the largest. This pattern has been considered as having been present in the non-mammaliaform cynodonts, such as *Thrinaxodon* (Crompton and Jenkins 1968), but only well-developed in early mammaliaforms such as *Sinoconodon* and *Morganucodon* (Crompton and Jenkins 1968; Crompton 1974; Kielan-Jaworowska et al. 2004). Eutriconodontans retain this general cusp-in-line pattern of the triconodontid tooth (Martin et al. 2020). In the study of the groups with triconodontid tooth pattern, tooth occlusion during chewing can be inferred from tooth wear; in particular, the occlusal relationship and the motion of the mandibular dentition are evidenced by wear facets on the upper teeth (Jäger et al. 2019). At least two distinct types of tooth occlusion are well-established in eutriconodontans.

In triconodontids (Fig. 8), there is a one-to-one tooth occlusion pattern in which the upper molariform cusp A occludes between cusps a and c of the corresponding lower molariform, and cusp a of the lower molariform occludes between cusps A and B of the corresponding upper molariform (Kielan-Jaworowska et al. 2004; Jäger et al. 2022). This occlusal pattern is comparable to that in *Morganucodon* (Crompton and Jenkins 1968; Crompton 1974; Kielan-Jaworowska et al. 2004) and the morganucodontan *Cifellilestes ciscoensis* (Davis et al. 2022). On the other hand, gobiconodontids (Jenkins and Crompton 1979; Jenkins and Schaff 1988; Kielan-Jaworowska and Dashzeveg 1998) display a two-to-one or embrasure tooth occlusion, resembling that of *Megazostrodon* (Mills 1971; Crompton 1974; Jenkins and Crompton 1979; Fig. 8). The tooth wear in both *G. zofiae* and *G. gongzhulingensis* are consistent with the gobiconodontid embrasure occlusal pattern. As discussed above, this occlusal relationship is critical for determining tooth count and dental formula.

In triconodontids, including gobiconodontids, molariforms are proportionally long, with cusp B/b, C/c, and D/d increasing in size relative to cusp A/a. This leads to a more uniform size among the three main cusps, with cusp D/d also increasing in size (Jäger et al. 2022; Fig. 8). As a result, the mesiodistally linear cutting crests of the teeth are lengthened, enhancing their cutting capabilities. The upper and lower teeth maintain a narrow transverse shape, with steep or nearly vertical wear facets and striations following a consistent orientation. This molariform morphology restricts directional changes, resulting in a single-phase power stroke (phase I) (Jäger et al. 2020; Fig. 8).

In *Gobiconodon*, the occlusal wear pattern suggests a pronounced labiolingually directed component of relative displacement between the lower and upper dentitions, as evidenced by the transverse wear groove developed on the upper molariforms. This groove records the passage of the central lower cusp a through the embrasure between

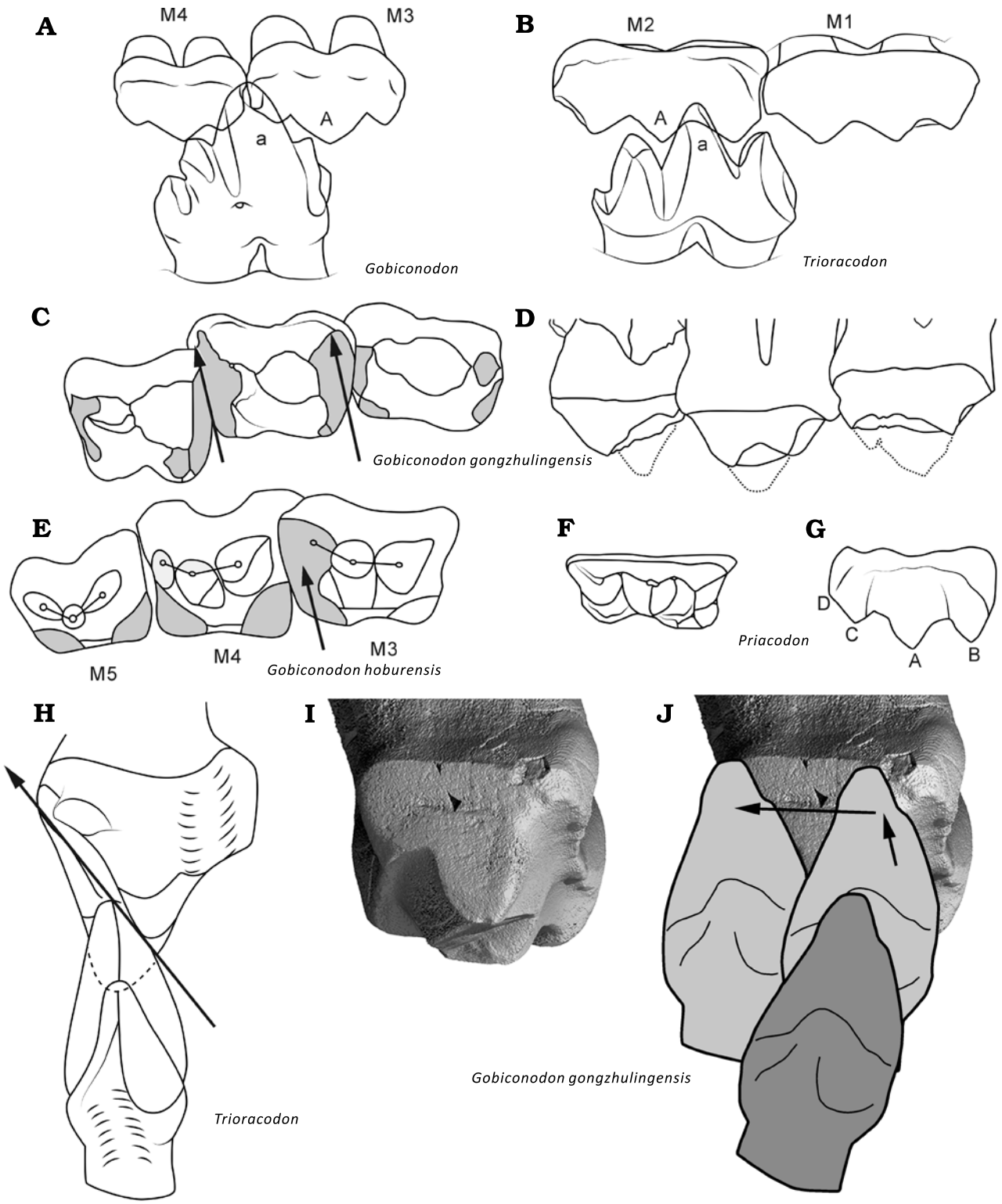

Fig. 8. Comparison of tooth occlusion and chewing movement of triconodontids and *Gobiconodon*. **A**. The two-to-one (embrasure) occlusion of *Gobiconodon*. **B**. The one-to-one occlusion of triconodontids (*Trioracodon*). Diagrams of occlusal (**C**) and labial (**D**) views of M2–4 of *G. gongzhulingensis* showing wear and widened crown and cusp shape. **E**. Diagram of occlusal view of M2–4 (our interpretation) of *Gobiconodon hoburensis* (Kielan-Jaworowska and Dash, 1998. Diagrams in occlusal (**F**) and labial (**G**) views of the upper molariform of a triconodontid (*Priacodon*); the tooth is scaled to the same length with M3 of *G. gongzhulingensis* to show the widened tooth crown of the latter. **H**. Distal view of the power stroke path presumably present in molariforms of triconodontids (Crompton and Jenkins 1968; Jäger et al. 2022). **I**. Distal view of M3 of *G. gongzhulingensis* showing the wear facet. **J**. The power stroke path (as indicated by the arrows and position of the lower tooth) presumably present in *G. gongzhulingensis.* A, B, F, H after Kielan-Jaworowska et al. (2004); E, after Kielan-Jaworowska and Dashzeveg (1998); I, J after Crompton and Jenkins (1968) and Jäger et al. (2020). Not to scale.

adjacent upper teeth, producing a labial-to-lingual shift of cusp a relative to the upper dentition during occlusion, as previously described for *G. ostromi* (Jenkins and Schaff 1988). A similar transverse groove is present in the upper molariforms of *G. borissiaki* (PSS 10-15b) and *G. hoburensis* (PSS IU37b). In these species, the tips of cusp a, b and c on ml are slightly worn horizontally, with no wear facets on the labial side, consistent with a labiolingually directed relative motion of cusp a within the embrasure during the power stroke (Jenkins and Schaff 1988; Kielan-Jaworowska and Dashzeveg 1998). This movement is further supported by the wear patterns of *G. gongzhulingensis* which bear horizontal striations perpendicular to the vertical axis or the roots of the teeth. Within an embrasure shearing framework, such striation orientations are interpreted as the result of an orthal closing movement of the mandible acting on inclined cusp and crown morphologies, which necessarily generates a labiolingually directed component of relative displacement between antagonistic teeth.

It can be inferred that in the early stages of ontogeny when the teeth of *G. gongzhulingensis* are unworn, cusp a of the lower molariform would occlude between two upper molariforms during food processing. A transverse groove is created at the embrasure by tooth wear, which extends labially while the tooth wear deepens. The embrasure wear groove indicates that during the orthal movement of the lower teeth, cusp a could fit in the labial end of the groove and travel a distance lingually, producing an effective transverse shearing component, during the power stroke. This contrasts with the one-phase chewing pattern of triconodontids. It is probable that the power stroke of *Gobiconodon* consists of two phases, an orthal one and a horizontal one (Fig. 8). In general, the triconodontid tooth contact and wear during the power stroke are on the labial (lower) and the lingual (upper) sides, whereas the contact is more on the mesial and distal sides of the molariforms in *Gobiconodon* and in a cusp-to-groove shearing relationship.

The development of transverse embrasure grooves in *Gobiconodo*n is facilitated by the transversely broadened upper molariforms. In a recent study, Mao et al. (2024; references therein) summarized three evolutionary pathways for the triconodont tooth pattern in a *Morganucodon*-like ancestor, presumably primitive, to give rise to other patterns by widening the cheek teeth by cusp semitriangulation and addition in docodontiforms, an addition of a cusp row in allotherians, and cusp triangulation and addition in holotherians. This widening process increases tooth ridges and wear facets, enhancing shearing and grinding efficiency during food processing. In *Gobiconodon*, molariform widening likewise increases wear facet area but is achieved primarily through inflation of the cusps rather than marked cusp rotation, triangulation, or the addition of new cusps. The flanking cusps are only moderately displaced, whereas the mesial and distal crests extending from the main cusps are distinctly oblique, providing effective guiding surfaces for transverse displacement during embrasure shearing. The incipient triangular arrangement of main cusps in some species of *Gobiconodon* (Kielan-Jaworowska and Dashzeveg 1998) likely lacks phylogenetic significance and may reflect a functional consequence of tooth widening, representing an evolutionary experiment for efficient chewing without the addition of new tooth cusps.

Triconodontids and *Gobiconodon* exhibit distinct types of tooth movement, possibly reflecting different diets. Simpson (1933: 135) considered triconodontids as “one of the most ideally carnivorous ever evolved” due to their dentition. However, detailed studies of tooth wear indicate that the dentition of triconodontids combines traits associated with carnivorous diets (because of the mesiodistally oriented cutting crests) and insectivorous diets (because of the bucco-lingually oriented crests and lobes), suggest a faunivorous diet including insects and small vertebrates rather than strictly carnivorous habits (Jäger et al. 2020). In contrast, the horizontal tooth movement of *Gobiconodon* suggests adaptation to an insectivorous or omnivorous diets rather than a purely carnivorous one, unlike the large carnivorous species of *Repenomamus*, which exhibits vertically oriented tooth wear facets due to the strong medial inclination of their molariforms (Hu et al. 2005; FM and JM personal observation). If *Volaticotherini* (Meng et al. 2006) is indeed a eutriconodontan group, it represents another form of tooth specialization and a possible faunivorous diet (Gaetano and Rougier 2011). The tooth shapes and wear patterns suggest diverse ecomorphological specializations and species diversification in eutriconodontans.

Conclusions

The combined study of *Gobiconodon zofiae* and the new species *Gobiconodon gongzhulingensis* provides a more comprehensive understanding of the gobiconodontidan *Gobiconodon*, such as a generalized formula of 2.1.2-3.5, with four upper molariforms consistently outnumbering the five lower ones, a pattern linked to embrasure occlusion. The two species demonstrate that tooth widening in *Gobiconodon* was achieved primarily through cusp inflation, not by pronounced cusp rotation or addition of new cusps, a distinct evolutionary pathway among eutriconodontans. Further, the late occurrence of *G. gongzhulingensis* extends the temporal range of *Gobiconodon* into the early Late Cretaceous of northeastern China, enriching the *Changchunsaurus* fauna and highlighting the genus’s prolonged persistence and wide paleobiogeographic distribution.

Acknowledgements

All authors are honored to have the paper published on the birthday of Prof. Zofia Kielan-Jaworowska (1925–2015). We thank Yemao Hou, Pengfei Yin, Jia Wang, Xiaomei Zhang (all IVPP) for CT scanning of the specimens, Aijuan Shi (IVPP) for drawing illustrations.

We sincerely thank Julia Schultz, Thomas Martin (both Universität Bonn, Germany) and Brian Davis (University of Louisville School of Medicine, USA) for their thorough and constructive comments and suggestions for improving this work. This research was supported by the National Key R&D Program of China (2025YFF0811700), the National Natural Science Foundation of China (42288201), the Project of China Geological Survey (WT2021036b) and the Youth Innovation Promotion Association CAS (Y2023017).

Editor: Eli Amson

References

Archibald, J.D. and Averianov, A.O. 2003. The Late Cretaceous placental mammal *Kulbeckia*. *Journal of Vertebrate Paleontology* 23: 404–419.

Averianov, A.O., Martin, T., Lopatin, A.V., Skutschas, P.P., Vitenko, D.D., Schellhorn, R., and Kolosov, P.N. 2023. On the way from Asia to America: eutriconodontan mammals from the Early Cretaceous of Yakutia, Russia. *The Science of Nature* 110: 40.

Averianov, A.O., Skutschas, P.P., Lopatin, A.V., Leshchinskiy, S.V., Rezvyi, A.S., and Fayngerts, A.V. 2005. Early Cretaceous mammals from Bol'shoi Kemchug 3 locality in West Siberia, Russia. *Russian Journal of Theriology* 4: 1–12.

Butler, P.M. and Clemens, W.A. 2001. Dental morphology of the Jurassic holotherian mammal *Amphitherium*, with a discussion of the evolution of mammalian post-canine dental formulae. *Palaeontology* 44: 1–20.

Butler, P.M. and Sigogneau-Russell, D. 2016. Diversity of triconodonts in the Middle Jurassic of Great Britain. *Palaeontologia Polonica* 67: 35–65.

Chen, J., Leblanc, A.R., Jin, L., Huang, T., and Reisz, R.R. 2018. Tooth development, histology, and enamel microstructure in *Changchunsaurus parvus*: implications for dental evolution in ornithopod dinosaurs. *PLoS One* 13(11): e0205206.

Chen, J., Mao, F.Y., Wu, W.H., and Meng, J. 2025. New material of the zalambdalestid *Zhangolestes* (Mammalia, Zalambdalestidae) from the Late Cretaceous *Changchunsaurus* Fauna of Jilin, China. *Acta Geologica Sinica-English Edition* 99: 634–645.

Chen, J., Richard, J.B., and Jin, L.Y. 2008. New material of large-bodied ornithischian dinosaurs, including an iguanodontian ornithopod, from the Quantou Formation (middle Cretaceous: Aptian-Cenomanian) of Jilin Province, northeastern China. *Neues Jahrbuch fur Geologie und Palaontologie-Abhandlungen* 248: 309–314.

Chow, M. and Rich, T.H. 1984. A new triconodontan (Mammalia) from the Jurassic of China. *Journal of Vertebrate Paleontology* 4: 226–231.

Clemens, W.A. and Lillegraven, J.A. 1986. New Late Cretaceous, North American advanced therian mammals that fit neither the marsupial nor eutherian molds. *Contributions to Geology Special Paper* 3: 55–85.

Crompton, A.W. 1974. The dentitions and relationships of the southern African Triassic mammals, *Erythrotherium parringtoni* and *Megazostrodon rudnerae*. *Bulletin of the British Museum (Natural History) Geology* 24 (7): 397–437.

Crompton, A.W. and Jenkins, F.A. 1968. Molar occlusion in Late Triassic mammals. *Biological Reviews* 43: 427–458.

Davis, B.M., Jäger, K.R.K., Rougier, G.W., Trujillo, K., and Chamberlain, K. 2022. A morganucodontan mammaliaform from the Upper Jurassic Morrison Formation, Utah, USA. *Acta Palaeontologica Polonica* 67: 77–93.

Gaetano, L.C. and Rougier, G.W. 2011. New materials of *Argentoconodon fariasorum* (Mammaliaformes, Triconodontidae) from the Jurassic of Argentina and its bearing on triconodont phylogeny. *Journal of Vertebrate Paleontology* 31: 829–843.

Hu, Y., Meng, J., Wang, Y., and Li, C. 2005. Large Mesozoic mammals fed on young dinosaurs. *Nature* 433: 149–152.

Huang, Q.H., Tan, W., and Yang, H.C. 1999. Stratigraphic succession and chronostrata of Cretaceous in Songliao basin. *Petroleum Geology & Oilfield Development in Daqing* 18 (6): 15–17, 28 [in Chinese with English abstract].

Jäger, K.R.K., Cifelli, R.L., and Martin, T. 2020. Molar occlusion and jaw roll in early crown mammals. *Scientific Reports* 10(1): 22378.

Jäger, K.R.K., Gill, P.G., Corfe, I., and Martin, T. 2019. Occlusion and dental function of *Morganucodon* and *Megazostrodon*. *Journal of Vertebrate Paleontology* 39 (3): e1635135.

Jäger, K.R.K., Gill, P.G., Martin, T., and Corfe, I.J. 2022. Molar morphology and occlusion of the Early Jurassic mammaliaform *Erythrotherium parringtoni*. *Acta Palaeontologica Polonica* 67: 975–982.

Jerzykiewicz, T., Currie P.J, Eberth, D.A., Johnston, P.A., and Zheng, J.J. 1993. Djadokhta Formation correlative strata in Chinese Inner Mongolia: an overview of the stratigraphy, sedimentary geology, and paleontology and comparisons with the type locality in the pre-Altai Gobi. *Canadian Journal of Earth Sciences* 30: 2180–2195.

Jenkins, F.A. and Crompton, A.W. 1979. Triconodonta. *In*: J.A. Lillegraven, Z. Kielan-Jaworowska, and W.A. Clemens (eds.), *Mesozoic Mammals: The First Two-thirds of Mammalian History*, 74–90. University of California Press, Berkeley.

Jenkins, F.A. Jr. and Schaff, C.R. 1988. The Early Cretaceous mammal *Gobiconodon* (Mammalia, Triconodonta) from the Cloverly Formation in Montana. *Journal of Vertebrate Paleontology* 8: 1–24.

Jin, L.Y., Chen, J., Zan, S.Q., and Godefroit, P. 2009. A new basal neoceratopsian dinosaur from the Middle Cretaceous of Jilin Province, China. *Acta Geologica Sinica-English Edition* 83: 200–206.

Jin, L.Y., Chen, J., Zan, S.Q., Richard, J.B., and Pascal, G. 2010. Cranial anatomy of the small ornithischian dinosaur *Changchunsaurus parvus* from the Quantou Formation (Cretaceous: Aptian–Cenomanian) of Jilin Province, northeastern China. *Journal of Vertebrate Paleontology* 30: 196–214.

Kermack, K.A., Mussett, F., and Rigney, H.W. 1973. The lower jaw of *Morganucodon*. *Zoological Journal of the Linnean Society* 53: 87–175.

Kermack, K.A., Mussett, F., and Rigney, H.W. 1981. The skull of *Morganucodon*. *Zoological Journal of the Linnean Society* 71: 1–158.

Kielan-Jaworowska, Z., Cifelli, R.L., and Luo, Z.X. 2004. *Mammals From the Age of Dinosaurs: Origins, Evolution, and Structure.* 630 pp. Columbia University Press, New York.

Kielan-Jaworowska, Z. and Dashzeveg, D. 1998. Early Cretaceous amphilestid ('triconodont') mammals from Mongolia. *Acta Palaeontologica Polonica* 43: 413–438.

Kielan-Jaworowska, Z., Hurum, J.H., and Badamgarav, D. 2003. An extended range of the multituberculate *Krytobaatar* and distribution of mammals in the Upper Cretaceous of the Gobi Desert. *Acta Palaeontologica Polonica* 48: 273–278.

Koenigswald, W. von, Anders, U., Engels, S., Schultz, J.A., and Kullmer, O. 2013. Jaw movement in fossil mammals: analysis, description and visualization. *Paläontologische Zeitschrift* 87: 141–159.

Kusuhashi, N., Wang, Y.Q., Li, C.K., and Jin, X. 2016. Two new species of *Gobiconodon* (Mammalia, Eutriconodonta, Gobiconodontidae) from the Lower Cretaceous Shahai and Fuxin formations, northeastern China. *Historical Biology* 28: 14–26.

Kusuhashi, N., Wang, Y.Q., Li, C.K., and Xun, J. 2020. New gobiconodontid (Eutriconodonta, Mammalia) from the Lower Cretaceous Shahai and Fuxin formations, Liaoning, China. *Vertebrata PalAsiatica* 58 (1): 45–66.

Li, C.K., Wang, Y.Q., Hu, Y.M., and Meng, J. 2003. A new species of *Gobiconodon* (Triconodonta, Mammalia) and its implication for the age of Jehol Biota. *Chinese Science Bulletin* 48: 1129–1134.

Li, J.L., Wang, Y., Wang, Y.Q., and Li, C.K. 2001. A new family of primitive mammal from the Mesozoic of western Liaoning, China. *Chinese Science Bulletin* 46: 782–785.

Linnaeus, C. 1758. *Systema naturae per regna tria naturae, secundum classes, ordines, genera, species, cum characteribus, differentiis, synonymis, locis. Vol. 1: Regnum animale.* Editio decima, reformata. 824 pp. Laurentii Salvii, Stockholm.

Lopatin, A.V. 2022. Direct evidence of the molariform tooth replacement in *Gobiconodon borissiaki* (Gobiconodontidae, Mammalia) from the Early Cretaceous of Mongolia. *Doklady Biological Sciences* 504: 73–77.

Lopatin, A. and Averianov, A. 2015. *Gobiconodon* (Mammalia) from the Early Cretaceous of Mongolia and revision of Gobiconodontidae. *Journal of Mammalian Evolution* 22: 17–43.

Mao, F.Y., Li, Z.Y., Wang, Z.L., Zhang, C., Rich, T., Vickers-Rich, P., and Meng, J. 2024. Jurassic shuotheriids show earliest dental diversification of mammaliaforms. *Nature* 628: 567–575.

Martin, T. and Schultz, J.A. 2023. Deciduous dentition, tooth replacement, and mandibular growth in the Late Jurassic docodontan *Haldanodon exspectatus* (Mammaliaformes). *Journal of Mammalian Evolution* 30: 507–531.

Martin, T., Jäger, K.R.K., Plogschties, T., Schwermann, A.H., Brinkkötter, J.J., and Schultz, J.A. 2020. Molar diversity and functional adaptations in Mesozoic mammals. *In*: T. Martin and W. von Koenigswald (eds.), *Mammalian Teeth—Form and Function*, 187–214. Verlag Dr. Friedrich Pfeil, Munich.

Maschenko, E.N. and Lopatin, A.V. 1998. First record of an Early Cretaceous triconodont mammal in Siberia. *Bulletin de l'Institut royal des sciences naturelles de Belgique, Sciences de la Terre* 68: 233–236.

Meng, J., Hu, Y.M., Wang, Y.Q., and Li, C.K. 2003. The ossified Meckel's cartilage and internal groove in Mesozoic mammaliaforms: implications to origin of the definitive mammalian middle ear. *Zoological Journal of the Linnean Society* 138: 431–448.

Meng, J., Hu, Y.M., Wang, Y.Q., and Li, C.K., 2005. A new triconodont (Mammalia) from the Early Cretaceous Yixian Formation of Liaoning, China. *Vertebrata PalAsiatica* 43: 1–10.

Meng, J., Hu, Y.M., Wang, Y.Q., Wang, X.L., and Li, C.K., 2006. A Mesozoic gliding mammal from northeastern China. *Nature* 444: 889–893.

Mills, J.R.E. 1971. The dentition of *Morganucodon*. *In*: D.M. Kermack and K.A. Kermack (eds.), Early Mammals. *Zoological Journal of the Linnean Society, London* 50 (Supplement 1): 29–63.

Rougier, G.W., Isaji, S., and Manabe, M. 2007. An Early Cretaceous mammal from the Kuwajima Formation (Tetori Group), Japan, and a reassessment of triconodont phylogeny. *Annals of Carnegie Museum* 76: 73–115.

Rougier, G.W., Novacek, M.J., McKenna, M.C., and Wible, J.R. 2001. Gobiconodonts from the Early Cretaceous of Oshih (Ashile), Mongolia. *American Museum Novitates* 3348: 1–30.

Rougier, G.W., Spurlin, B.K., and Kik, P.K. 2003. A new specimen of *Eurylambda aequicrurius* and considerations on "symmetrodont" dentition and relationships. *American Museum Novitates* 3398: 1–15.

Schultz, J.A. and Martin, T. 2014. Function of pretribosphenic and tribosphenic mammalian molars inferred from 3D animation. *Naturwissenschaften* 101 (10): 771–781.

Sigogneau-Russell, D. 2003. Diversity of triconodont mammals from the Early Cretaceous of North Africa-Affinities of the amphilestids. *Palaeovertebrata* 32: 27–55.

Simpson, G.G. 1933. Paleobiology of Jurassic mammals. *Palaeobiologica* 5: 127–158.

Trofimov BA. 1978. The first triconodonts (Mammalia, Triconodonta) from Mongolia. *Doklady Academii Nauk SSSR* 251: 209–212 [in Russian].

Ungar, P.S., 2015. Mammalian dental function and wear: a review. *Biosurface and Biotribology* 1 (1): 25–41.

Wan, X.Q., Zhao, J., Scott, R.W., Wang, P.J., Feng, Z.H., Huang, Q.H., and Xi, D.P. 2013. Late Cretaceous stratigraphy, Songliao Basin, NE China: SK1 cores. *Palaeogeography, Palaeoclimatology, Palaeoecology* 385: 31–43.

Wang, G.D., Cheng, R.H., Wang, P.J., Gao, Y.F., Wang, C.S., Ren, Y.G., and Huang, Q.H. 2009. Description of Cretaceous sedimentary sequence of the Quantou Formation recovered by CCSD-SK-Is borehole in Songliao Basin: lithostratigraphy, sedimentary facies and cyclic stratigraphy. *Earth Science Frontiers* 16: 324–338.

Wang, L.H., Li, X.B., and Chen, J. 2022a. Theropods materials and their variety in *Changchunsaurus* fauna and its diversity. *Journal of Jilin University (Earth Science Edition)* 52 (6): 1844–1854. [In Chinese]

Wang, L.H., Tian, Y.K., and Zhao, J.J. 2020. A rapid hydroclimate change and its influence on the Songliao Basin during the Santonian-Campanian transition as recorded by compound-specific isotopes. *Palaeogeography, Palaeoclimatology, Palaeoecology* 546: 109674.

Wang, P.J., Du, X.D., Wang, J., and Wang, D.P. 1996. The chronostratigraphy and stratigraphic classification of the Cretaceous of the Songliao Basin. *Acta Geologica Sinica (English Edition)* 9: 207–217.

Wang, Q., Zan, S.Q., Jin, L.Y., and Chen, J. 2006. A new oospecies, *Dictyoolithus gongzhulingensis*, from the Early Cretaceous Quantou Formation in the central Jilin Province. *Journal of Jilin University (Earth Science Edition)* 36: 153–157.

Wang, T.T., Ramezani, J., Wang, C.S., Wu, H.C, He, H.Y., and Bowring, S.A. 2016. High-precision U–Pb geochronologic constraints on the Late Cretaceous terrestrial cyclostratigraphy and geomagnetic polarity from the Songliao Basin, Northeast China. *Earth and Planetary Science Letters* 446: 37–44.

Wang, T.T., Yang, C.S., Ramezani, J., Wan, X.Q., Yu, Z.Q., Gao, Y.F., He, H.Y., and Wu, H.C. 2022b. High-precision geochronology of the Early Cretaceous Yingcheng Formation and its stratigraphic implications for Songliao Basin, China. *Geoscience Frontiers* 13: 101386.

Wang, X.R. 2005. *Theropoda Teeth of Early Cretaceous from Quantou Formation in Gongzhuling, Jilin Province.* 46 pp. MSc. Thesis, Jilin University, College of Earth Science, Changchun.

Wang, Y.Q., Hu, Y.M., Meng, J., and Li, C.K. 2001. An ossified Meckel's cartilage in two Cretaceous mammals and origin of the mammalian middle ear. *Science* 294: 357–361.

Wu, W.H., Dong, Z.M., Sun, Y.W., Li, C.T., and Li, T. 2006. A new sauropod dinosaur from the Cretaceous of Jiutai, Jilin, China. *Global Geology* 25: 6–9.

Xi, D.P., Wang, X.Q., Li, G.B., and Li, G. 2019. Cretaceous integrative stratigraphy and timescale of China. *Science China: Earth Sciences* 62: 256–286.

Xu, X., Tan, Q.W., Wang, S., Sullivan, C., Hone, D., Han, F.L., Ma, Q.Y., Tan, L., and Xiao, D. 2013. A new oviraptorid from the Upper Cretaceous of Nei Mongol, China, and its stratigraphic implications. *Vertebrata PalAsiatica* 51 (2): 85–101.

Yang, L., Li, X.B., Chen, J., and Reisz, R.R. 2023. First discovery of large-bodied dromaeosaurid fossil materials (Dinosauria: Theropoda) from the Upper Cretaceous Quantou Formation, Songliao Basin, Northeast China. *Cretaceous Research* 153: 105711.

Yuan, C.X., Xu, L., Zhang, X.L., Xi, Y.H., Wu, Y.H., and Ji, Q. 2009. A new species of *Gobiconodon* (Mammalia) from western Liaoning, China and its implication for the dental formula of *Gobiconodon*. *Acta Geologica Sinica-English Edition* 83: 207–211.

Zan, S.Q., Jin, L.Y., Chen, J., and Xu, Y. 2003. Discovery of Cretaceous Dinosaur Fauna in Central Jilin and Its Significance. *Journal of Jilin University (Earth Science Edition)* 33: 119–120.

Zan, S.Q., Wood, C.B., Rougier, G.W., Jin, L., Chen, J., and Schaff, C.R. 2006. A new "middle" Cretaceous zalambdalestid mammal, from a new locality in Jilin Province, northeastern China. *Journal of the Paleontological Society of Korea* 22: 153–172.

Zhu, J.C., Feng, Y.L., Meng, Q.R., Li S., Wu, G.L, and Zhu, R.X. 2020. Decoding stratigraphic and structural evolution of the Songliao Basin: Implications for late Mesozoic tectonics in NE China. *Journal of Asian Earth Sciences* 194: 104138.